

Discriminating fluvial fans and deltas: Channel network morphometrics reflect distinct formative processes

Luke Gezovich^{1*}, Piret Plink-Björklund¹, Jack Henry^{1,2}

¹ Colorado School of Mines, Geology & Geologic Engineering, 1500 Illinois Street, Golden, CO, 80401

² Rice University, Earth, Environmental and Planetary Sciences, 6100 Main St., Houston, TX, 77005-1827

Correspondence to: Luke Gezovich (lukegezovich@mines.edu)

Abstract

Recent recognition of a new type of fluvial system – fluvial fans – introduces a fan-shaped channel network that appears similar to that of river-dominated deltas. Deltas form where rivers enter lakes and oceans, while fluvial fans are terrestrial landforms. However, fluvial fans can reach the shorelines of oceans or lakes, and in such cases the distinction between fluvial fan and river-dominated delta channel networks becomes ambiguous. We currently lack fundamental understanding of these two landforms’ morphometric differences, despite their high socioeconomic significance, vulnerability to natural hazards, and key differences in how these landforms respond to global climate change and urbanization. Here we review the relevant conceptual differences in delta and fluvial fan network morphodynamics, propose a set of quantitative morphometric criteria to distinguish fluvial fan and delta channel networks, and test these criteria on 40 deltas and 40 fluvial fans from across the world. This initial attempt to contrast and distinguish deltas and fluvial fans based on their channel network morphometrics demonstrates that quantifying channel network angles (mean of 73.8° for deltas and 55.0° for fluvial fans), and trends in normalized channel widths and lengths provide efficient criteria, but some ambiguities remain that need to be resolved in future work. This research advances our mechanistic understanding of fluvial fan and delta channel networks and the recognition of modern and ancient landforms on Earth and other planetary bodies, such as Mars and Saturn’s moon Titan.

Deleted: ,

Plain Language Summary

Fluvial fans are a newly recognized type of river system that look like river deltas, especially when they reach lakes or oceans. This study explores how to tell them apart by measuring the size and layout of channels in these fan-shaped landforms. Understanding these differences helps to predict how these landforms respond to climate change and urbanization, and to identify them on Mars and other planetary bodies.

38 1. Introduction

39 River deltas are depositional landforms that form where rivers enter lakes or oceans. They are
40 home to over half a billion people, host abundant and biodiverse ecosystems, and function as both
41 economic and agricultural hubs (Saito et al., 2007; Tejedor et al., 2015). The form and function of deltas
42 is intimately linked to the evolving structure of their channel networks that determine how deltas
43 distribute sediment and nutrients (Passalacqua, 2017; Pearson et al., 2020; Tejedor et al., 2017). Delta
44 channel network morphology results from an intricate balance between sediment erosion and deposition
45 from river, tide, and wave energy fluxes. River fluxes create distributary channels and islands, tides
46 roughen the shoreline and widen the channels, and waves smooth the shoreline and decrease the number
47 of distributary channels (Broaddus et al., 2022; Galloway, 1975; Nienhuis et al., 2015, 2018; Paniagua-
48 Arroyave & Nienhuis, 2024; Vulis et al., 2023). Deltas dominated by river energy fluxes (river-dominated
49 deltas) (Broaddus et al., 2022; Galloway, 1975; Nienhuis et al., 2015, 2018; Paniagua-Arroyave &
50 Nienhuis, 2024; Vulis et al., 2023) characteristically form fan-shaped landforms with complex
51 distributary channel networks (Fig. 1). In these deltas, channel network topology is defined by mouth bar
52 deposition and consequent distributary channel bifurcation (Bates, 1953; Edmonds & Slingerland, 2007;
53 Wright, 1977). To specifically refer to these deltaic processes, we define “bifurcations” as a process
54 related to mouth bar deposition and consequent channel branching.

55 Fluvial fans are another type of fan-shaped landform with channel networks that share
56 morphological similarities with the river-dominated delta channel networks (Fig. 2). Fluvial fans are a
57 relatively newly acknowledged type of fluvial landform (Ventra & Clarke, 2018; Weissman et al., 2010),
58 which forms via river avulsions or “channel jumps” across low-gradient floodplains (Chakraborty et al.,
59 2010; Martin & Edmonds, 2023; North & Warwick, 2007). Rivers have been traditionally regarded as
60 sediment transfer or bypass zones in source-to-sink systems (Allen, 2008; Fielding et al., 2012), whereas
61 fluvial fans are net depositional and build significant stratigraphic thicknesses (Chakraborty et al., 2010;
62 Moscariello, 2018; Weissmann et al., 2015). Fluvial fans are also called “wet” fluvial-dominated alluvial
63 fans (Schumm, 1977), megafans (Singh et al., 1993), or distributive fluvial systems (DFS) (Weissman et
64 al., 2010). Fluvial fans are distinct landforms from alluvial fans – which form by a combination of
65 gravitational and streamflow processes, feature steep gradients (typically 2–12°), and have a relatively
66 small radius typically less than 10 km (Blair & McPherson, 1994; Moscariello, 2018). Fluvial fans form
67 some of the largest terrestrial landforms on Earth (10³–10⁵ km² in surface area) (Horton & Decelles, 2001;
68 Leier et al., 2005) and have low gradients (typically 0.03–0.001°) (Brooke et al., 2022). Fluvial fans are
69 abundant across Earth, and they form in diverse climatic and tectonic settings (Hartley et al., 2010; Ventra
70 & Clarke, 2018; Weissmann et al., 2010).

Deleted: (Saito et al., 2007; Tejedor et al., 2015).

Deleted: (Galloway 1975; Nienhuis et al 2015; 2018; Broaddus et al 2022; Vulis et al 2023; Paniagua-Arroyave and Nienhuis 2024)

Deleted: (Bates, 1953; Edmonds & Slingerland, 2007; Wright, 1977). ...

Commented [PP1]: I think we need something here upfront to avoid confusion

Formatted: Font color: Auto

Deleted: that

Deleted: (Weissman et al., 2010).

79 Like deltas, fluvial fans are home to hundreds of millions of people, and these highly dynamic
80 landforms are critical for their livelihood – supporting agriculture, fisheries, and freshwater access. For
81 example, the Kosi fluvial fan experiences catastrophic river floods that lead to large numbers of casualties
82 and displaced populations (Sinha, 2009; Syvitski & Brakenridge, 2013). While fluvial fans are terrestrial
83 landforms, they can reach the shorelines of oceans (Fig. 2b) or lakes (Figs. 2a, 2d and 2i). In such cases
84 the distinction between fluvial fan and river-dominated delta channel networks becomes ambiguous,
85 while wave- and tide-dominated deltas have distinctly recognizable morphologies (Broaddus et al., 2022;
86 Galloway, 1975; Nienhuis et al., 2015; 2018; Paniagua-Arroyave & Nienhuis, 2024; Vulis et al., 2023).
87 We currently lack quantitative morphometric criteria for distinguishing river-dominated delta and fluvial
88 fan channel networks, despite their socioeconomic significance, key differences in their natural hazard
89 vulnerabilities, and in how they respond to global change. Deltas are global change hotspots highly
90 vulnerable to urbanization and climate change, which can aggravate coastal hazards and cause sea level
91 rise (Giosan et al., 2014; Syvitski et al., 2009), and reduce sediment supply due to river damming and
92 artificial levees, causing the drowning of deltas (Blum & Roberts, 2009; Giosan et al., 2014; Nienhuis et
93 al., 2020; Paola et al., 2011; Syvitski et al., 2009).

94 Numerous fan-shaped landforms with channel networks have also been identified on other planetary
95 bodies such as Mars (Malin & Edgett, 2015; Ori et al., 2000; Wood, 2006) and Saturn’s moon Titan
96 (Radebaugh et al., 2018; Wall et al., 2010; Witek & Czechowski, 2015). Deltas on planetary bodies are
97 important indicators of paleo-shorelines and have been utilized to reconstruct the shorelines and water
98 levels of ancient lakes and oceans on Mars (Di Achille & Hynek, 2010). However, Martian paleo-ocean
99 shoreline reconstructions have so far yielded mixed results (De Toffoli et al., 2021). This discrepancy
100 could perhaps arise because shoreline-bound deltas have not been effectively distinguished from fluvial
101 fans on Mars, which may form thousands of kilometers inland from shorelines (Bramble et al., 2019;
102 Limaye et al., 2023; Tebolt & Goudge, 2022). Deltas also offer attractive targets for mission sites in
103 search of life due to their habitability and high biosignature preservation potential, as exemplified by the
104 selection of Jezero Crater for NASA’s *Perseverance* rover, *Ingenuity* helicopter, and future Mars Sample
105 Return mission (Farley et al., 2020). Distinguishing deltaic and fluvial fan paleo-channel networks on
106 other planetary bodies is even more ambiguous, especially if the lakes and oceans are no longer present.

107 Over time, the accumulation of biogenic and sedimentary materials distributed via channel networks
108 contributes to the construction of stratigraphy. Fluvial fans and deltas are net depositional systems, as
109 both are characterized by spatially diminishing water surface slopes that reduce sediment transport
110 capacity, thereby producing spatiotemporal convergence and deposition of sediment (Ganti et al., 2014).
111 Consequently, in addition to their socioeconomic significance, both landforms significantly contribute to
112 the stratigraphic record, and their deposits can be used to decipher past environmental conditions. High

Deleted: (Hartley et al., 2010; Weissman et al., 2010; Ventra & Clarke, 2018).

Deleted: It is i

Deleted: distinction

Deleted:

Deleted: s

119 deposition rates in fluvial fans and deltas promote the preservation of environmental change signals in the
120 sedimentary record (Trampusch & Hajek, 2017). Similar to modern river-dominated deltas and fluvial
121 fans, we lack morphometric criteria to distinguish these two fan-shaped channel networks in the
122 sedimentary record, such as in seismic datasets.

123 This study is motivated by developing quantitative morphometric distinction criteria for fluvial fan
124 and river-dominated delta channel networks. Prior work has established quantitative morphological
125 criteria for describing deltaic channel networks and linked these characteristics to theory (Chen et al.,
126 2021; Coffey & Shaw, 2017; Edmonds et al., 2011; Edmonds & Slingerland, 2007; Fagherazzi et al.,
127 2015; Ke et al., 2019; Passalacqua, 2017; Pearson et al., 2020; Tejedor et al., 2015, 2017). However, there
128 are no existing quantitative criteria to characterize fluvial fan channel networks or to differentiate the two
129 landforms. To develop such criteria, we review the relevant conceptual differences in delta and fluvial fan
130 network morphodynamics, propose quantitative morphometric criteria to distinguish fluvial fan and delta
131 channel networks, and test these criteria on 40 deltas and 40 fluvial fans (Supplementary Data) from
132 across the globe (Fig. 3). We test the robustness of the approach by analyzing differences in channel
133 network morphometrics concerning the size and gradient of the systems, hydroclimate conditions, lake
134 versus ocean terminations and tide versus wave influences in deltas, and channel morphology in fluvial
135 fans. We assess how effectively the proposed methods distinguish fluvial fans from river-dominated
136 deltas and examine why this distinction matters under global change. This work serves to improve our
137 mechanistic understanding of fluvial fan and delta evolution, and their accurate recognition on Earth,
138 other planetary bodies, and in the sedimentary record.

139 2. Delta and Fluvial Fan Channel Network Morphodynamics

140 The nature of channel networks is dependent on distinct morphodynamic processes responsible for
141 their formation (Edmonds & Slingerland, 2007; Fagherazzi et al., 2015; Tejedor et al., 2015). Below we
142 analyze differences in delta and fluvial fan morphodynamics and review existing morphometric criteria
143 for quantifying deltaic distributary channel networks. Our review is not comprehensive; rather, it focuses
144 on the specific processes that govern the formation of the morphometric characteristics that we can then
145 use for distinction of these two landforms, namely channel network angles, and downstream changes in
146 channel widths and lengths. There are other important characteristics of deltaic channel networks, linked
147 to water and sediment discharge distribution, entropy, and connectivity (Chen et al., 2021; Ke et al., 2019;
148 Passalacqua, 2017; Pearson et al., 2020; Tejedor et al., 2015, 2017). These aspects are not considered in
149 this review, because they are outside the scope of this study that seeks to distinguish deltaic and fluvial
150 fan channel networks using easily applicable morphometric criteria that can be used for both deltaic and
151 fluvial fan networks.

Deleted: -

Deleted: -

Deleted: ¶

Deleted: (Edmonds & Slingerland, 2007; Fagherazzi et al., 2015; Tejedor et al., 2015).

Deleted: which

Deleted: to

159 We use the terms bifurcation and avulsion as *processes* rather than a geomorphological feature of
160 channel splitting. *Bifurcation* is the process of channel splitting driven by mouth bar formation (Edmonds
161 & Slingerland, 2007). *Avulsions* are channel “jumps”, where a channel changes its course due to channel
162 super-elevation or a more favorable (steeper) gradient at channel flanks (Gearon et al., 2024; Jones &
163 Schumm, 1999; Slingerland & Smith, 2004). Partial avulsions split channels; however, the process is
164 distinct from *bifurcation* around a mouth bar.

165 2.1 River Deltas

166 Deltas (Fig. 1) form only where a river enters a standing body of water. Here, the transport capacity
167 of the turbulent jet decreases, and the “parent” stream jet flow experiences both lateral and bed friction,
168 causing the flow to decelerate and rapidly expand laterally (Bates, 1953; Edmonds & Slingerland, 2007;
169 Jerolmack & Swenson, 2007; Wright, 1977). As a result, the transport capacity of the turbulent jet
170 decreases and sediment is deposited as a mouth bar basinward of the river mouth (Edmonds &
171 Slingerland, 2007). The process of mouth bar deposition and growth eventually leads to the bifurcation, or
172 downstream branching of a single (parent) channel into two daughter channels (Axelsson, 1967; Coffey &
173 Shaw, 2017; Edmonds & Slingerland, 2007) (Fig. 4a). These daughter channels are separated by an island
174 or shallow bay where sediment transport is significantly reduced or nonexistent, and flow is
175 unchannelized (Coffey & Shaw, 2017). Mouth bar deposition and resultant channel bifurcation repeat
176 multiple times, leading to the seaward advancement of the shoreline and the construction of a delta
177 distributary channel network (Edmonds & Slingerland, 2007; Olariu & Bhattacharya, 2006) (Fig. 4a).

178 Deltas also experience channel avulsions at the lobe-level (Slingerland & Smith, 2004). These deltaic
179 avulsions occur within a region of high-water surface slope variability caused by backwater
180 hydrodynamics that are characterized by spatial flow deceleration and deposition during low flows, and
181 flow acceleration and bed scour with high flows (Brooke et al., 2022; Chatanantavet et al., 2012;
182 Chatanantavet & Lamb, 2014). As the backwater zone sets the location for avulsion in deltas
183 (Chatanantavet et al., 2012), they are strongly controlled by hydrodynamics in their receiving basin, like
184 bifurcations. As a result, the delta lobe size is generally consistent and the lobe avulsion node migrates
185 downstream commensurate with shoreline progradation (Ganti et al., 2014). as influenced by flood
186 frequency, sediment supply, or sea-level rise (Brooke et al., 2022). These avulsions episodically rearrange
187 the depocenter at the delta lobe scale, whereas the substantially more frequent bifurcations generate the
188 topology of the delta distributary channel networks (Bentley et al., 2016; Edmonds & Slingerland, 2007).

189 Resultant delta channel networks have a specific angle at which distributary channels bifurcate (Fig.
190 4a) (Coffey & Shaw, 2017). because a channel bifurcation will grow toward an equilibrium angle of 72°
191 to maximize flux at the two channel tips (Coffey & Shaw, 2017; Devauchelle et al., 2012; Ke et al., 2019;
192 Mahon et al., 2024). First described in tributary networks, this theoretical angle arises from diffusive

Deleted: (Edmonds & Slingerland, 2007).

Deleted: -

Deleted: (Gearon et al., 2024; Jones & Schumm, 1999a; Slingerland & Smith, 2004)

Deleted: (Gearon et al., 2024).

Deleted: ¶

Deleted: always

Deleted: the mouth of

Deleted: (Bates, 1953; Wright, 1977; Edmonds & Slingerland, 2007; Jerolmack & Swenson, 2007).

Deleted: (Edmonds & Slingerland, 2007).

Deleted: (Axelsson, 1967; Coffey & Shaw, 2017; Edmonds & Slingerland, 2007)

Deleted: (Coffey & Shaw, 2017).

Deleted: (Olariu & Bhattacharya, 2006; Edmonds & Slingerland, 2007) ...

Deleted: (Slingerland & Smith, 2004).

Deleted:

Deleted: (Lamb et al., 2012; Brooke et al., 2022); Chatanantavet & Lamb, 2014).

Deleted: (Chatanantavet et al., 2012),

Deleted: (Ganti et al., 2014)

Deleted: although recent work by

Deleted: shows that changes in flood frequency, sediment supply, or sea-level rise can also shift avulsion nodes upstream or downstream

Deleted: (Edmonds & Slingerland, 2007; Bentley et al., 2016). ¶

Deleted: (Coffey & Shaw, 2017),

222 groundwater flow (Devauchelle et al., 2012). Testing of this concept reports bifurcation angles of $70.4^\circ \pm$
 223 2.6° (n = 9) in natural deltas (Coffey & Shaw, 2017), and $68.3^\circ \pm 8.7^\circ$ (n = 21) (Coffey & Shaw, 2017)
 224 and $74.1^\circ \pm 7.7^\circ$ (n = 13) (Federici & Paola, 2003) in experimental deltas.

Deleted: (Devauchelle et al., 2012).
 Deleted: (Coffey & Shaw, 2017),
 Deleted: and
 Deleted: (Coffey & Shaw, 2017) <object><object>and
 Deleted: ;

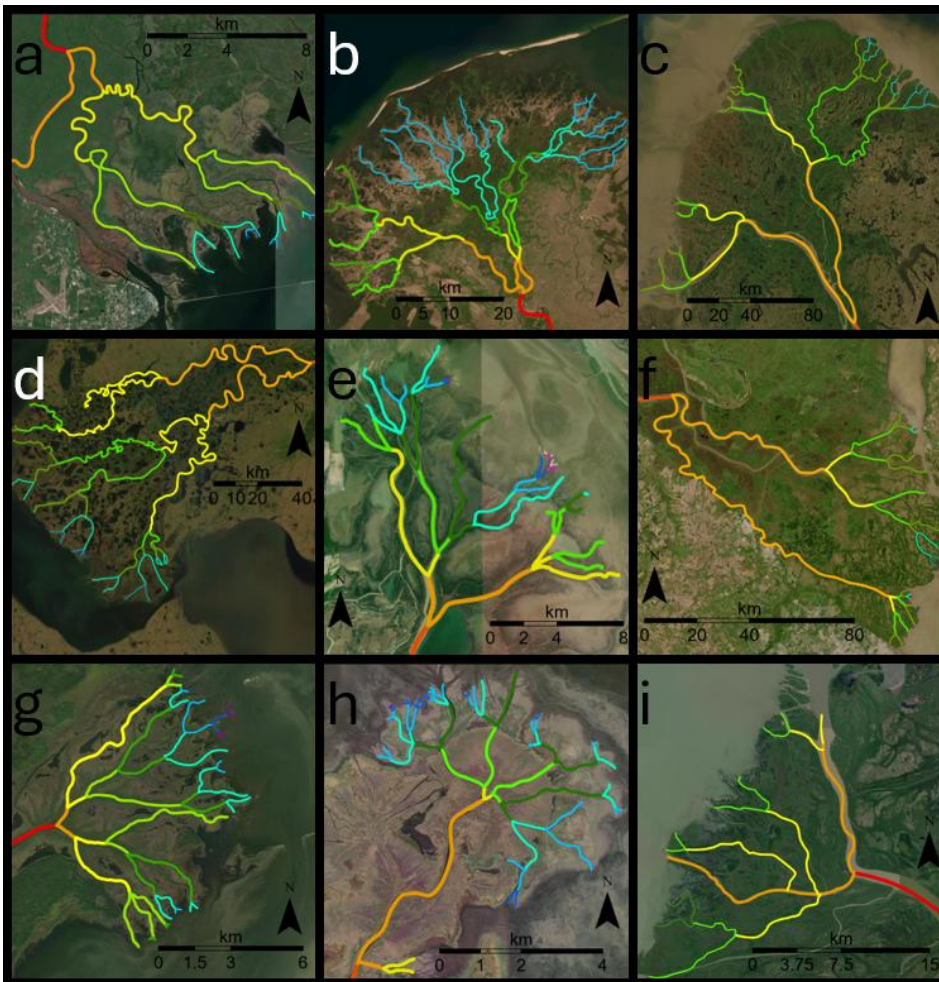


Figure 1: Examples of delta channel networks: (a) Apalachicola, (b) Selenga, (c) Yukon, (d) Kobuk, (e) Poyang Lake, (f) Parana (g) Saskatchewan, (h) Mamawi lake, (i) Slave deltas. The colors indicate channel hierarchy (see Methods). Base imagery from Esri's World Imagery basemap (© Esri, Maxar, Earthstar Geographics, and the GIS User Community).

225 Deltaic channel networks tend to consistently self-organize (Edmonds et al., 2011; Fagherazzi, 2008)
 226 and exhibit a theoretical fractal pattern of decreasing channel widths and lengths associated with
 227 increasing bifurcation order (Edmonds et al., 2011; Edmonds & Slingerland, 2007; Hariharan et al., 2022;

Deleted: ¶
 Deleted: ¶

320 Seybold et al., 2017; Wolinsky et al., 2010) (Fig. 4a). Edmonds & Slingerland, (2007) show that channel
321 width trends align with hydraulic geometric scaling: as the discharge of a parent channel divides into the
322 discharge for two resultant daughter channels, the daughter channel dimensions decrease as they scale
323 with bankfull discharge. Channel lengths decrease downstream with each successive bifurcation because
324 the jet momentum flux and consequent average grain transport distance decrease downstream, causing
325 new mouth bar deposition and accompanying bifurcations to occur closer to the previous bifurcation node
326 for a given channel (Edmonds & Slingerland, 2007) (Figs. 4a and 5a).

Formatted: Not Highlight

327 The nature of delta channel networks is further affected by waves and tides (Broaddus et al., 2022;
328 Geleynse et al., 2011; Jerolmack & Swenson, 2007), where the relative strength of river, wave, and tide
329 processes determines whether deltas are river, wave, or tide dominated (Galloway, 1975; Nienhuis et al.,
330 2015, 2018; Paniagua-Arroyave & Nienhuis, 2024; Vulis et al., 2023). Since wave- and tide-dominated
331 deltas exhibit distinct morphologies from river-dominated delta and fluvial fan channel networks, they are
332 not considered in this study (See Methods for more information on classification).

Deleted: (Jerolmack & Swenson, 2007; Geleynse et al., 2011; Broaddus et al., 2022),

Deleted: (Galloway, 1975; Nienhuis et al 2015, 2018; Nienhuis et al., 2020a; Vulis et al 2023; Paniagua-Arroyave and Nienhuis, 2025).

Deleted: derived because of difference processes

333 2.2 Fluvial Fans

334 In contrast to deltas where bifurcations and avulsions are strongly controlled by hydrodynamics near
335 a receiving basin of standing water (Brooke et al., 2022; Chatanantavet et al., 2012; Ganti et al., 2014),
336 fluvial fan river avulsions are driven by a topographic slope break (Ganti et al., 2014; Martin & Edmonds,
337 2023). Increased likelihood of avulsions at the fan apex is a consequence of the gradient reduction that
338 triggers in-channel sediment aggradation (Parker et al., 1998). These avulsions result from high channel
339 bed aggradation rates that are considerably higher than on the surrounding floodplains (Pizzuto, 1987).
340 This process causes river channel superelevation which ultimately triggers river avulsions near the fan
341 apex (Bryant et al., 1995; Gearon et al., 2024; Mohrig et al., 2000). Since this slope break controls the
342 location of the fluvial fan's apex, the avulsion node is thus topographically pinned (Ganti et al., 2014), at
343 this abrupt change in gradient, unlike in deltas (Brooke et al., 2022). Partial or full avulsions do occur
344 further downfan, involving local gradient or discharge decreases, or crevassing processes (Assine, 2005;
345 Chakraborty et al., 2010; Donselaar et al., 2013; Gearon et al., 2024) (Fig. 2).

Deleted:

Deleted: (Chatanantavet et al., 2012; Ganti et al., 2014)

Deleted: (Ganti et al., 2014; Martin and Edmonds, 2023).

Deleted:

Deleted: (Parker et al., 1998)

Deleted: (Pizzuto, 1987).

Deleted: (Bryant et al., 1995; Mohrig et al., 2000; Gearon et al 2024).

Deleted: (Ganti et al., 2014)

Deleted: (Assine, 2005; Chakraborty et al., 2010; Donselaar et al., 2013; Gearon et al 2024)

Deleted: from

Formatted: Indent: First line: 0.25"

Deleted: that

Deleted: (North & Warwick, 2007)

346 Fluvial fan channel networks result through repeated nodal style avulsions that typically shift the
347 primary river to different regions of the fan (Slingerland & Smith, 2004). These avulsions superimpose
348 new channel positions on paleo-channel locations and can split channels by partial avulsions and
349 crevasses. This generates apparent channel "bifurcations" (North & Warwick, 2007) (Fig. 4b). However,
350 as a process, these are not bifurcations related to mouth bar deposition but rather generated by avulsions.
351 Fluvial fan channel networks are predominantly paleo-channel networks rather than active channel

409 networks like in deltas (Chakraborty et al., 2010; North & Warwick, 2007). Multiple channels can
 410 actively transmit discharge at partial avulsions, such as during major river floods.

Deleted: (North & Warwick, 2007; Chakraborty et al., 2010)....

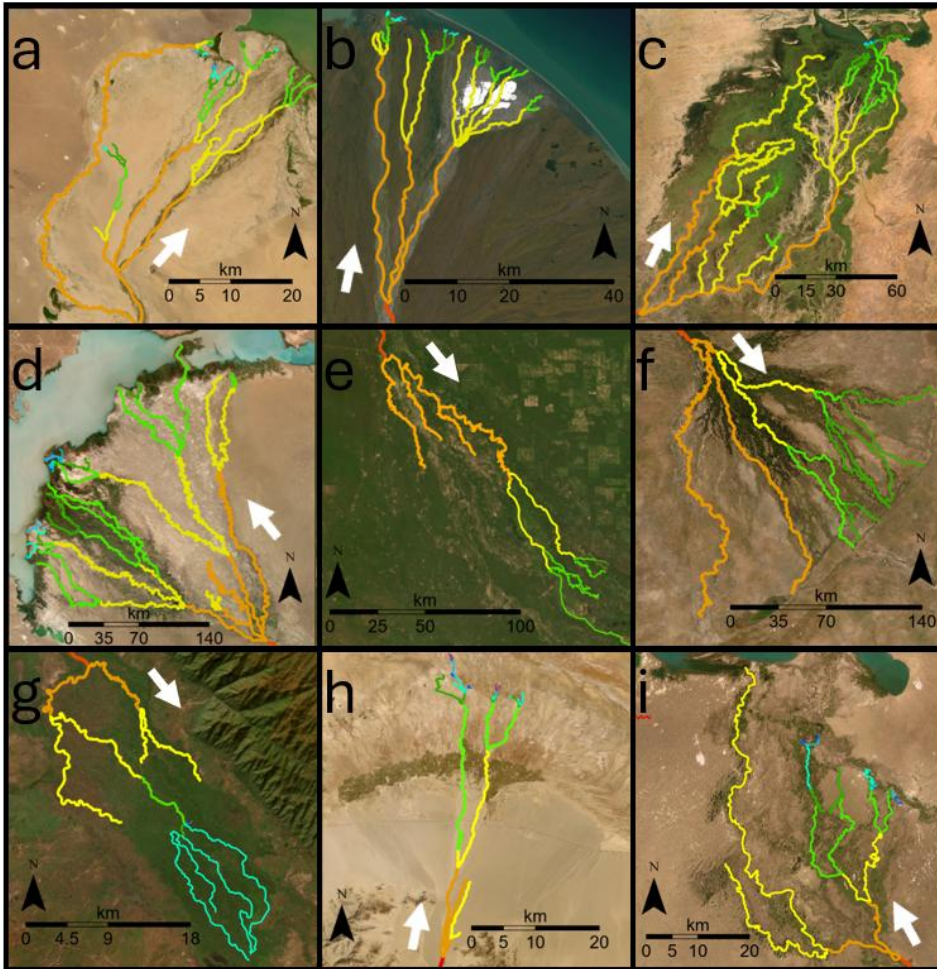


Figure 2: Examples of fluvial fan channel networks: (a) Dzavhan Gol, (b) Kongakut, (c) Niger, (d) Ili, (e) Pilcomayo, (f) Okavango, (g) Shire, (h) Nomon He, and (i) Aksu fans. The colors indicate channel hierarchy (see Methods), and white arrows indicates downfan direction. Base imagery from Esri's World Imagery basemap (© Esri, Maxar, Earthstar Geographics, and the GIS User Community).

411 Downfan decreases in channel width have been well documented in modern and ancient fluvial fans
 412 (Davidson et al., 2013; Kelly & Olsen, 1993; Nichols, 1987; Nichols & Fisher, 2007; Owen et al., 2015;
 413 Wang & Plink-Björklund, 2019; Weissman et al., 2010). linked to discharge losses to floodplain
 414 processes, infiltration into the loose sediments of the fan, and evapotranspiration (Davidson et al., 2013;

Deleted: .

Formatted: Font: (Default) Times New Roman, 11 pt

Formatted: Font: (Default) Times New Roman, 11 pt

Deleted: <object>

Deleted: ¶

¶
 ¶
 ¶
 Downstream ...

Deleted: s

Deleted: (Nichols, 1987; Kelly & Olsen, 1993; Nichols & Fisher, 2007; Weissman et al., 2010; Davidson et al., 2013; Owen et al., 2015; Wang & Plink-Björklund, 2019),

427 Hartley et al., 2010; Horton & Decelles, 2001; Weissman et al., 2010). However, some fluvial fan
 428 channels have also been shown to widen downstream, possibly due to changes in channel planform or
 429 aspect ratio, discharge contribution from groundwater, or discharge capture from adjacent rivers
 430 (Chakraborty et al., 2010; Davidson et al., 2013). Fluvial fan channel networks have been studied for
 431 qualitative descriptions of channel planform morphology (Davidson et al., 2013; Hartley et al., 2010;
 432 Weissman et al., 2010) and scaling relationships (Davidson et al., 2013; Davidson & Hartley, 2014).
 433 Modeling establishes a relationship between the fluvial fan shape and avulsion dynamics, like avulsion
 434 trigger period and abandoned channel dynamics (Edmonds et al., 2022; Martin & Edmonds, 2023).
 435 Fluvial fans are distinct landforms from alluvial fans that feature steep gradients (typically 2–12°),
 436 have a relatively small radial distance typically less than 10 kilometers, and lack channel networks (Blair
 437 & McPherson, 1994; Moscariello, 2018). Although surface channels may occur on alluvial fans, these are
 438 transient features formed by surface erosion, and do not construct alluvial fans, which form by a
 439 combination of gravitational and sheet flood processes (Blair & McPherson, 1994; Moscariello, 2018).
 440 Thus, alluvial fans are not considered here as they are distinct from fluvial fan channel networks that form
 441 by river avulsions.

Deleted: (Horton & Decelles, 2001; Hartley et al., 2010; Weissman et al., 2010; Davidson et al., 2013).

Deleted: (Chakraborty et al., 2010; Davidson et al., 2013).

Deleted: ,

Deleted: such as

Deleted: (Edmonds et al., 2022; Martin & Edmonds, 2023). ¶

Formatted: Font:

442 2.3 Morphometric Criteria for Recognition of Delta and Fluvial Fan Channel Networks

Deleted: ¶

443 Based on the above differences in delta and fluvial fan morphodynamics, we hypothesize that the
 444 morphometric differences in their channel networks can be quantified. Based on prior work, we expect
 445 river-dominated delta channel networks to display downstream decreasing channel widths and lengths
 446 with increasing bifurcation order (Edmonds & Slingerland, 2007; Seybold et al., 2007; Wolinsky et al.,
 447 2010) and have an average channel network angle of approximately 72° (Coffey & Shaw, 2017). These
 448 metrics should differ in fluvial fans, because the channel networks are built by avulsions rather than
 449 bifurcations. However, delta networks also experience avulsions, and we expect some overlap in the
 450 network angles. Below, we test these morphometric criteria on 40 river-dominated delta and 40 fluvial fan
 451 channel networks (Fig. 3).

Deleted: H.

Deleted: (Edmonds & Slingerland, 2007; Seybold et al., 2007; Wolinsky et al., 2010),

Deleted: (Coffey & Shaw, 2017).

Deleted: also

Deleted: avulsions

Deleted: ¶

452 3. Dataset and Methods

453 Although automated channel mapping tools like ChannelExtractor in TopoToolbox (Schwanghart &
 454 Kuhn, 2010) and Rivamap (Isikdogan et al., 2017) exist, these methods rely on either terrain-based flow
 455 routing or the detection of active surface water, typically based on spectral characteristics, to delineate
 456 river channels. However, fluvial fan channel networks are predominantly composed of paleo-channels
 457 that lack both clear topographic expression and surface water signatures. Both delta and fluvial fan
 458 channels can also be only a few meters wide, often falling below the spatial resolution of commonly
 459 available DEMs and remote sensing imagery. In such settings, the coarse resolution and smoothing of

Deleted: Although

Formatted: Indent: First line: 0.25"

Deleted: existing

Deleted:

Deleted: –

Deleted:

Deleted: –

481 subtle terrain in DEMs, especially in low-relief environments, further limit the effectiveness of automated
482 extraction. As a result, we are constrained to manual digitization, as described below.

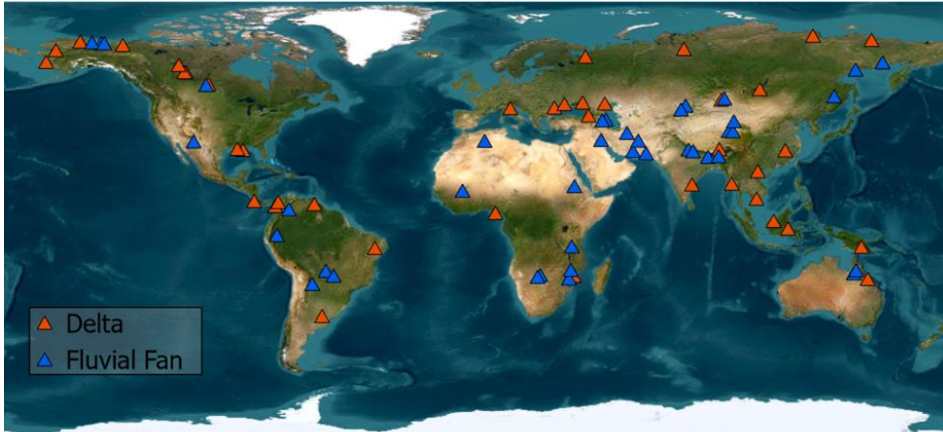


Figure 3: Map of deltas and fluvial fans in this study. Base imagery from Esri's World Imagery basemap (© Esri, Maxar, Earthstar Geographics, and the GIS User Community).

483 3.1 Channel Order

484 To establish channel order in networks, we follow (Dong et al., 2016). Their method follows a simple
485 rule: bifurcations produce downstream increasing channel order through channels that branch. To be
486 considered a channel of a higher order, the resultant channels must not merge downstream. When a first-
487 order channel bifurcates, two second-order channels develop downstream of this bifurcation. When these
488 two channels subsequently bifurcate, two new pairs of third-order channels form, and so on (Figs. 4a and
489 4b). All channels from the first instance of branching up to and include those that enter a body of water or
490 terminate on land are measured. Identification of bifurcation nodes follows Edmonds et al., (2011), such
491 that the first-order bifurcation for a river channel is the first bifurcation that the channel undergoes (Fig.
492 4a). Although these methods were developed for deltaic channel networks, here we adapt them for fluvial
493 fan networks also (Figs. 4c and 4d). We do not map or measure channels that loop or rejoin downstream,
494 or channels of non-fluvial origin, such as tidal channels or inlets (Smart, 1971; Tejedor et al., 2015) that
495 are not connected to the fluvial distributary channels. We also omit local avulsions, on fluvial fans, which
496 generate channels that typically merge downfan (Slingerland & Smith, 2004). Paleo-channels on fluvial
497 fans were recorded where possible. Paleo-channels resembled active channels that exhibit little to no
498 discharge when we mapped the channel networks. We included paleo-channel measurements in fluvial
499 fans because they are ubiquitous in fluvial fans (Hartley et al., 2010), and many of these channels do carry
500 discharge if reactivated during major flood events.

501 3.2 Channel Length and Width Measurements

Formatted: Font color: Auto

Deleted: ¶

Deleted: Dong et al. (2016).

Formatted: Indent: First line: 0.25"

Deleted: (

Deleted: Edmonds et al. (2011),

Deleted: consider

Deleted: (e.g., Smart, 1971; Tejedor et al., 2015)

Deleted: (Slingerland & Smith, 2004)

Deleted:

Deleted: ¶

511 Channel length and width measurements follow Edmonds & Slingerland (2007), where channel
512 length is measured as the distance between two bifurcation nodes in deltas (Fig. 4a). We adopt this
513 methodology also to fluvial fans to measure channel lengths between avulsion nodes (Fig. 4c). The
514 average width of a channel segment is recorded from three separate width measurements: one
515 immediately after a node (w_i), one immediately before the next node (w_i), and one halfway between these
516 two points at the midpoint of the channel segment (w_h) (Figs. 4a and 4c). Channel width measurements
517 were not performed in locations where a channel has locally split into multiple branches that join
518 downstream. In deltas, channel width measurements were recorded based on the width of water present in
519 the channel, as observed in the satellite imagery. For fluvial fans, paleo-channel width measurements
520 were based on the bankfull width, defined by clearly visible channel banks or vegetation boundaries. All
521 channel width measurements were normalized using the initial first-order channel width, following the
522 methodology of Edmonds & Slingerland (2007). Consequently, the normalized channel width value for
523 first-order channels is always equal to one. First-order channel lengths were measured between the last
524 occurrence of tributary channels and the first channel splitting node and contain no significant value for
525 our study. All channel length measurements (l) were also normalized using the first order channel width
526 measurements according to existing methodologies (Edmonds & Slingerland, 2007; Jerolmack, 2009). As
527 such, the normalized first order channel length values merely reflects our selected methodologies rather
528 than an attributable morphological characteristic.

529 3.3 Network Angle Measurements

530 To quantify network angles, we adopt the methodology of Coffey & Shaw (2017) developed for
531 measuring channel bifurcation angles, which determines the angles of mouth bars formed at the end of an
532 upstream channel. In this methodology, the final channel width directly upstream of a bifurcation (w_i) is
533 set as the length for two limbs of an angle that follows the mouth bar-water contact to measure a
534 bifurcation angle (θ_n) (Coffey & Shaw, 2017) (Fig. 4b). The same methodology is adapted here for fluvial
535 fans (Fig. 4d). In some river deltas, tidal processes cause bifurcation of a channel into three channels
536 instead of two; these are referred to as trifurcations (Leonardi et al., 2013), furcation (Shaw et al., 2018)
537 or polyfurcations (Chamberlain et al., 2018), and a few such measurements are included in the dataset in
538 the very distal portions of deltas where tidal influence is significant. We do not measure angles where
539 channels loop or rejoin downstream of avulsions or bifurcations. In essence, we focus on the morphology
540 of branching channel networks and measure the visible angles between channels or paleo-channels
541 independent of their origin (Fig. 4b and 4d).

Deleted: (
Deleted: ,
Deleted: Edmonds and Slingerland (2007),
Formatted: Indent: First line: 0.25"

Deleted: length and
Deleted: (
Deleted: Edmonds & Slingerland (2007).

Deleted: ¶
Deleted: (
Formatted: Normal, Indent: Left: 0", First line: 0.25"

Deleted: (Coffey & Shaw, 2017)

Deleted: (Leonardi et al., 2013)

Deleted: ¶
Formatted: Font: (Default) Times New Roman, Bold

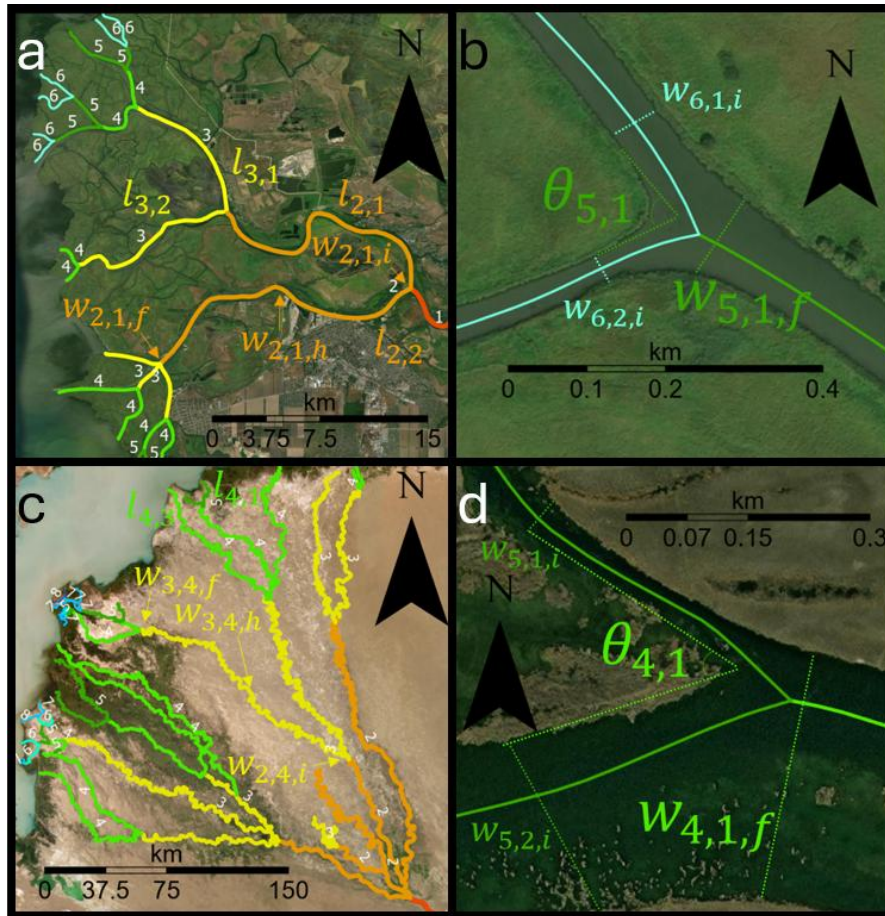


Figure 4: Illustration of (a) channel order, length, and width and (b) bifurcation angle measurements in deltas (Don delta). Illustration of (c) channel order, length, and width and (d) divergence/crossover angle measurement (Ili fan). Arrows point to locations of w_i = initial channel width, w_h = midpoint channel width, w_f = final width measurements. The w_f is set as the length of two limbs that track along the edges of the mouth bar. θ_n corresponds to the bifurcation or divergence/crossover order. Base imagery from Esri's World Imagery basemap (© Esri, Maxar, Earthstar Geographics, and the GIS User Community).

554 3.4 Global Delta and Fluvial Fan Channel Network Database

555 To test the applicability of the proposed criteria, we selected 40 river-dominated deltas and 40
 556 fluvial fans (Fig. 3 and Supplementary Data) to be mapped using composite satellite data (ESRI, 2025).
 557 These landforms were selected from a diverse range of hydroclimatic, topographic, and basinal conditions
 558 from across the world (Fig. 3). Only river-dominated deltas are included in the dataset, because wave-and

559 ~~tide-dominated delta morphology is distinct from that of fluvial fans.~~ All deltas have been identified as
 560 such by prior work (Broaddus et al., 2022; Galloway, 1975; Hartley et al., 2010; Leier et al., 2005;
 561 Nienhuis et al., 2015, 2018; Vulis et al., 2023), ~~and display active discharge based on satellite imagery.~~
 562 The river dominance of deltas and the presence of tide- or wave-influence was determined using the
 563 established principles of process-based delta classification (Broaddus et al., 2022; Galloway, 1975;
 564 Nienhuis et al., 2015, 2018; Paniagua-Arroyave and Nienhuis ~~2024~~; Vulis et al., 2023). ~~However,~~
 565 ~~categorical discrepancies exist between these different classification approaches. To clarify our~~
 566 ~~terminology,~~ we define “dominated” versus “influenced” deltas as follows. Wave-dominated deltas (e.g.
 567 São Francisco, Eel) are characterized by strandplanes and a complete absence of bifurcations; these deltas
 568 are excluded from our study. Wave-influenced deltas still possess morphological features such as
 569 strandplains, but exhibit clear, measurable channel bifurcations and are included in our study. Similarly,
 570 tide-dominated deltas (e.g. Fly, Yangtze) have a limited number of channels that widen substantially
 571 seaward, whereas tide-influenced deltas such as the Yukon (Fig. 1c) exhibit channel widening ~~only in the~~
 572 ~~most distal channels~~ (Xu & Plink-Björklund, 2023). ~~In practice, we combine these parameters with~~
 573 ~~established classifications~~ (Broaddus et al., 2022; Galloway, 1975; Nienhuis et al., 2015, 2018; Paniagua-
 574 Arroyave & Nienhuis, 2024; Vulis et al., 2023) ~~to categorize the deltas in our study. Please refer to the~~
 575 ~~Supplementary Data for information regarding our classification of each delta.~~ We test the effects of tide-
 576 and wave-influence on the morphometric criteria by comparative analyses.

577 Fluvial fans were located using their apex coordinates from the global fluvial fan database of
 578 Hartley et al., (2010). This database also includes data on fluvial fan length, gradient, termination style
 579 (e.g. axial, contributory, lacustrine, marine, playa, desert/dune, and wetland). ~~Termination styles refer to~~
 580 ~~the environment where the fluvial fan terminates: for instance, a contributory termination style denotes~~
 581 ~~that the landform channels switch from distributary to contributory at the toe of the fan, while axial fans~~
 582 ~~are classified when the main channel forms a confluence with an axial fluvial system (Hartley et al.,~~
 583 ~~2010).~~ We also subdivided delta termination styles in lakes and oceans. To test the robustness of our
 584 methodology, we analyze whether the landform size, gradient, termination style, or wave- and tide-
 585 influence in deltas affect the results.

586 3.5 Mapping with ArcGIS Pro

587 Delta and fluvial fan channel networks were mapped using ArcGIS Pro software (Version 3.2.1)
 588 (Fig. 1, 2, and 4). Two feature classes were created: one for deltas and one for fluvial fans. Each delta or
 589 fluvial fan landform was then individually mapped as a shapefile layer under the corresponding feature
 590 class. The shapefiles for channel networks were created as polyline features, which allow users to
 591 manually trace individual river channel segments while automatically recording line lengths. Channel
 592 widths and angles were measured using the line and angle measurement tools in ArcGIS Pro. All data ~~was~~

Deleted:

Deleted: .

Deleted: 2025

Deleted: All included deltas display active discharge based on satellite imagery. Only river-dominated deltas are included in the dataset, because wave-and tide-dominated delta morphology is distinct from that of fluvial fans.

Deleted: ies

Deleted: may

Deleted: only minor

Deleted: in this study

Deleted: Many natural river-dominated deltas are, however, tide- or wave-influenced to varying extents.

Formatted: Font:

Deleted: (

Deleted: Hartley et al. (2010).

Deleted:

Deleted: , such as

Deleted: styles

Deleted: C

Deleted:

Deleted: refers

Deleted: to

Deleted: es

Deleted: a distributive paleo-channel pattern becomes contributory at the fan toe, and

Deleted: to

Deleted: where

Deleted: active

Deleted: s

Deleted: another

Deleted: river

Deleted: (Hartley et al., 2010)

Formatted: Font:

Deleted: ¶

Deleted: a

Deleted: s

Deleted: was

629 recorded in the attribute table for each landform. This data was organized into Excel documents and
630 subsequently converted to Python- and Pandas- readable CSV files (Supplementary Data).

Deleted: then exported and ...rganized into Excel documents and subsequently converted to a...Pp...thon- and Pp...

631 ~~One~~ limitation of our methodology is ~~uncertainty regarding the timing of~~ satellite image
632 ~~acquisition relative to~~ precipitation events. ~~Precipitation increases~~ channel discharge, ~~thereby increasing~~
633 measured channel widths, ~~particularly for~~ fluvial fans in arid environments. Such events can also
634 reactivate partial avulsions and crevasses, ~~which can~~ potentially increase the apparent number of
635 channels. However, none of the selected systems exhibited observable seasonal or ~~large-scale~~ discharge
636 changes across their channel networks ~~attributable to different timings in data collection~~. Additionally,
637 because this study relies on values normalized to the initial channel width, the effects of seasonal
638 variability on channel width measurements are minimized.

Deleted: A... limitation of our methodology is the uncertainty regarding how ...he timing soon ...f satellite image acquisition relative to s were captured after a precipitation events. for a given landform, ...recipitation which can significantly ...ncreases influence ...hannel discharge, and ...hereby affect ...ncreasing measured channel widths, especially ...articularly in ...or arid ...luvia fans in arid environments. Such events can also reactivate partial avulsions and crevasses, which can potentially increasing. ...the apparent number of channels. However, none of the selected systems exhibited observable seasonal or significant ...arge-scale discharge changes across their channel networks attributable to different timings in data collection.....

639 3.6 Code and Statistics

640 Kolmogorov-Smirnov and Shapiro-Wilk tests were first applied to determine whether the data ~~are~~
641 normally distributed. Levene's test was used to test ~~differences in variances of~~ populations ~~that~~ do not
642 exhibit a normal distribution. (Trauth, 2006). ~~Independent samples or Welch's t-test~~ were then applied to
643 test for a difference in means for populations with similar and dissimilar variances, respectively, while
644 one-sample ~~t-tests~~ were used to test comparisons of a subgroup against the overall population mean
645 (Trauth, 2006). For this study, a p-value less than 0.05 (5% significance level) suggests that the two
646 population distributions, variances, or means are not similar. Data ~~confidence intervals~~ were calculated
647 according to ~~Mendenhall et al., (2012)~~. Data analysis and visualization were performed using Python.
648 Open-source data visualization libraries Matplotlib (Hunter, 2007), ~~NumPy~~ (Harris et al., 2020), ~~SciPy~~
649 (Virtanen et al., 2020), ~~and Seaborn~~ (Waskom, 2021), were utilized.

Deleted: is ...re normally distributed. Levene's test was used to test for ...ifferences in variances in ...f populations which ...hat do not exhibit a normal distribution (Trauth, 2006). (Trauth, 2006). ...ndependent samples or Welch's t...test were then applied to test for a difference in means for populations with similar and dissimilar variances, respectively, while one-sample T...-tests were used to test comparisons of a subgroup against the overall population mean (Trauth, 2006). (Trauth, 2006). ... or this study, a p-value less than 0.05 (5% significance level) suggests that the two population distributions, variances, or means are not similar. Data analyses ...onfidence intervals were calculated according to (...endenhall et al., (2012). Mendenhall et al., (2012). ...ata analysis and visualization were performed using Python. Open-source data visualization libraries Matplotlib (Hunter, 2007), (Hunter, 2007), ...umPy (Harris et al., 2020), (Harris et al., 2020), ...ciPy (Virtanen et al., 2020), (Virtanen et al., 2020) ...nd Seaborn (Waskom, 2021)...(Waskom, 2021)

650 4. Results

651 4.1 Delta and Fluvial Fan Channel Network Angles

652 The ~~mean~~ channel network angle (θ_a) in deltas is 73.8° with a 95th percentile confidence interval of \pm
653 1.9° ($n = 528$) (Fig. 5a). The ~~mean~~ channel network angle (θ_f) in fluvial fans is $55.0^\circ \pm 2.0^\circ$ ($n = 520$)
654 (Fig. 5b). The delta and fluvial fan network angle populations are not normally distributed according to
655 both Kolmogorov-Smirnov (KS) and Shapiro-Wilk (SW) tests, with p-values less than 0.05. Levene's test
656 for statistical difference in variances also results in a p-value less than 0.05, suggesting population
657 variances are statistically different. A subsequent independent sample ~~t-test~~ suggests the means of delta

Formatted: Font color: Text 1

Deleted: ¶

Deleted: average ...ean channel network angle (θ_a) in deltas is 73.8° with a 95th percentile confidence interval of $\pm 1.9^\circ$ ($n = 528$) (Fig. 5a). The average ...ean channel network angle (θ_f) in fluvial fans is $55.0^\circ \pm 2.0^\circ$ ($n = 520$) (Fig. 5b). The delta and fluvial fan network angle populations are not normally distributed according to both Kolmogorov-Smirnov (KS) and Shapiro-Wilk (SW) tests, with p-values less than 0.05. Levene's test for statistical difference in variances also results in a p-value less than 0.05, suggesting population variances are statistically different. A subsequent independent samples...T

747 and fluvial fan angle populations are statistically different, with a p-value less than 0.05. All statistical
 748 results are recorded in Supplementary Table 1 in the Supplementary Information.
 749

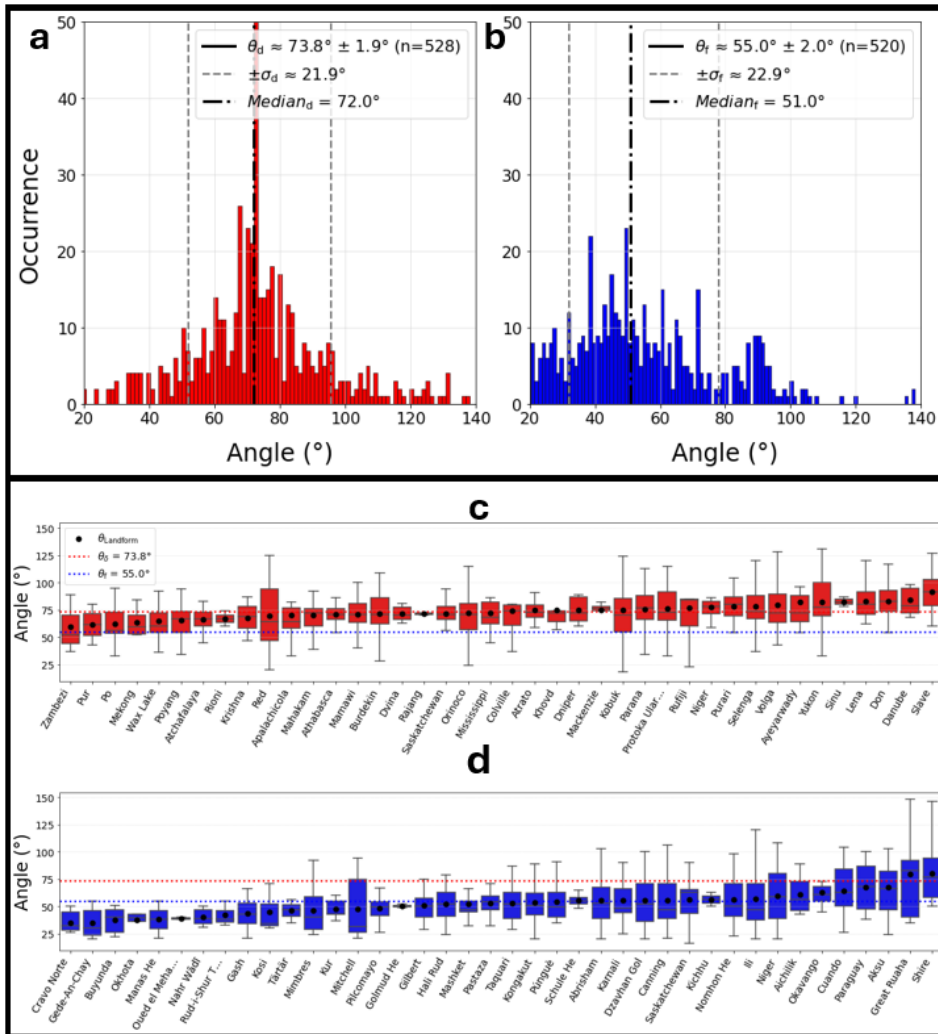


Figure 5: Histograms depicting distributions of (a) delta angles with mean delta angle (θ_d), its standard deviation (σ_d) and median and (b) fluvial fan angles with mean fan angle (θ_f), its standard deviation (σ_f), and median displayed. Box-and-whisker plot displaying the mean angle for each delta (c) and fluvial fan (d) landform ($\theta_{Landform}$).

Deleted: average

Deleted:

Deleted: average

Deleted:

Deleted: average

781 angle for the 19 river-dominated deltas ($\theta_R = 73.4^\circ \pm 2.2^\circ$, $n = 375$), for the 16 tide-influenced deltas ($\theta_T =$
 782 $75.6^\circ \pm 3.9^\circ$, $n = 139$), and for the 5 wave-influenced deltas ($\theta_W = 67.1^\circ \pm 10.1^\circ$, $n = 14$) (Fig. 7a). The
 783 river-dominated and tide-influenced delta angle means are not statistically different from the mean angle
 784 for the whole delta population (Supplementary Table 1). The wave-influenced delta angles were omitted
 785 from this statistical analysis due to a small sample size ($n = 14 < 30$).

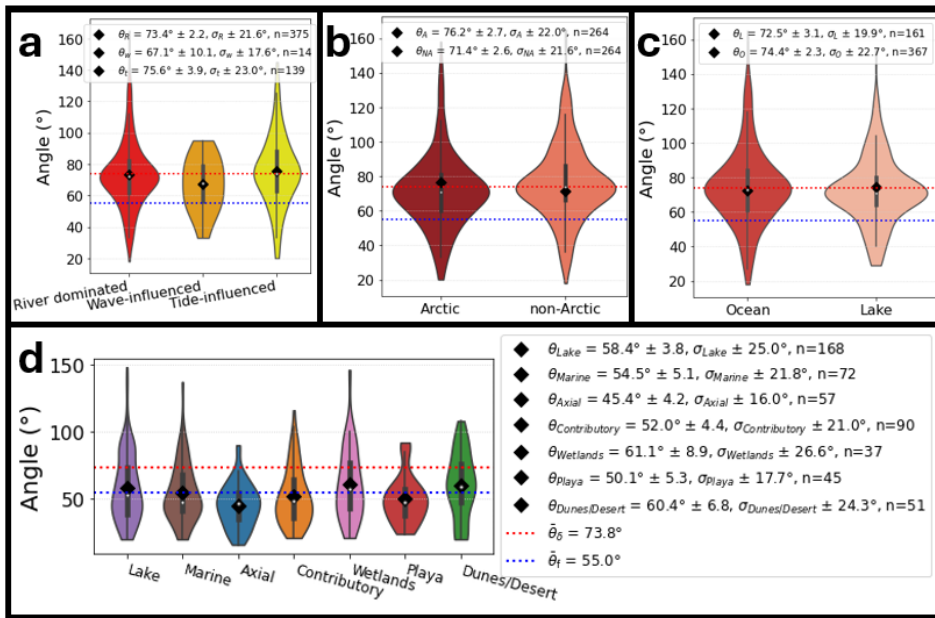


Figure 7: Violin plots depicting angle distributions for (a) delta process regime: river dominated (θ_R), wave-influenced (θ_W), and tide-influenced (θ_T), (b) deltas in non-Arctic (θ_{NA}) and Arctic (θ_A) climates, (c) ocean terminated deltas (θ_O) and lake terminating deltas (θ_L), and (d) fluvial fan termination styles. All mean angle values have a corresponding 95th percent confidence intervals, standard deviation (σ), and sample count (n).

786 Many delta angle measurements in this dataset come from Arctic deltas. The comparison between
 787 Arctic and non-Arctic deltas shows that Arctic deltas have a larger mean angle ($\theta_A = 76.2^\circ \pm 2.7^\circ$, $n =$
 788 264) than non-Arctic deltas ($\theta_{NA} = 71.4^\circ \pm 2.6^\circ$, $n = 264$) (Fig. 7b). There is a statistically significant
 789 difference in means between Arctic and non-Arctic deltas (Supplementary Table 1). Grouping deltas by
 790 termination style (Fig. 7c) shows that lake-terminating deltas have slightly smaller mean angles than those
 791 that terminate in oceans ($\theta_L = 72.5^\circ \pm 3.1^\circ$, $n = 161$ versus $\theta_O = 74.4^\circ \pm 2.3^\circ$, $n = 367$), but these
 792 differences are not statistically significant compared to the whole delta population (Supplementary Table
 793 1).

794 Grouping fluvial fans by their termination style shows some differences (Fig. 7d), where the mean

Deleted:)
 Deleted: is
 Deleted: (
 Deleted:)
 Deleted:
 Deleted: (
 Deleted:)
 Deleted: (
 Deleted: <object>

Deleted: average

Deleted: ¶

867 angles vary from a low of $\theta_{\text{Axial}} = 45.4^\circ \pm 4.2^\circ$ (n = 57) for axial-terminating fluvial fans to $\theta_{\text{wetlands}} = 61.1^\circ$
868 $\pm 8.9^\circ$ (n = 37) for ~~wetland~~-terminating fans (Fig. 7d). All fluvial fan termination types, except for axial-
869 terminating fans, exhibit population means that are statistically similar to the overall fluvial fan
870 population (Supplementary Table 1). However, each termination style is represented by only 4 to 6
871 landforms, limiting the statistical power of comparisons and generalizations, despite the relatively robust
872 measurement numbers in wetland (n = 37), playa (n = 45), dunes/desert (n = 51), and axial-terminating
873 fans (n = 57). There also appears to be some discrepancies in ~~Hartley et al., (2010)'s~~ assignment of
874 termination types, ~~such as referring to playa fans as lacustrine or ocean fans as contributory~~. We also
875 tested whether landform size (Supplementary Fig. 1) and gradient (Supplementary Fig. 2) affect the
876 channel network angles, and these analyses yield no trends, supporting the robustness of our
877 methodology.

878 4.2 Channel Lengths and Widths

879 Normalized channel length and width measurements reveal morphological differences between
880 fluvial fan and delta channels. Both landform types show non-linear decreases in these values with
881 increasing channel order (Fig. 8). Statistical analyses confirm that the overall means for normalized
882 channel length and width differ significantly between fluvial fans and deltas (Supplementary Table 1).
883 Fluvial fan channels are generally an order of magnitude longer than delta channels, with a mean
884 normalized length of 147.09, compared to 17.18 ~~for~~ deltas (Figs. 8a and 8c). In contrast, delta channels
885 tend to be slightly wider, with a mean ~~normalized~~ width of 0.40 compared to 0.26 ~~for~~ fluvial fans (Figs.
886 8b and 8d).

887 Comparing the normalized dimensions by channel order (Fig. 9) ~~reveals additional~~ trends. The
888 ~~normalized channel widths of lower-order fluvial fan channels~~ (orders 1–5) are significantly longer, and
889 the channel shortening rate is higher compared to deltas (Fig. 9a). The normalized lengths become very
890 similar in orders 7–8, then diverge again for the higher orders where the fluvial fan channel lengths are
891 somewhat longer, but the channel shortening rates are higher in deltas. Normalized channel widths show
892 significant differences for orders 2–8, but not for 9–11. Only a few landforms have channels with orders
893 exceeding 9. Fluvial fan narrowing rates are very high from order 1 and 2, and very low in orders 7–10
894 (Fig. 9b). The narrowing rates are more uniform in deltas.

895 When comparing individual deltas by process regime, ~~both~~ tide- and wave-influenced deltas have
896 ~~significantly~~ higher mean normalized channel widths relative to the ~~overall~~ delta population
897 (Supplementary Fig. 3 and Supplementary Table 1).

Deleted: wetland

Deleted: (

Deleted: Hartley et al. (2010)

Deleted:

Formatted: Indent: First line: 0.25"

Deleted: ,

Deleted: in

Deleted: normalized

Deleted: in

Deleted: shows

Deleted: further

Deleted: lower order

Deleted: in fluvial fans

Deleted: and

Deleted: a significantly

Deleted: whole

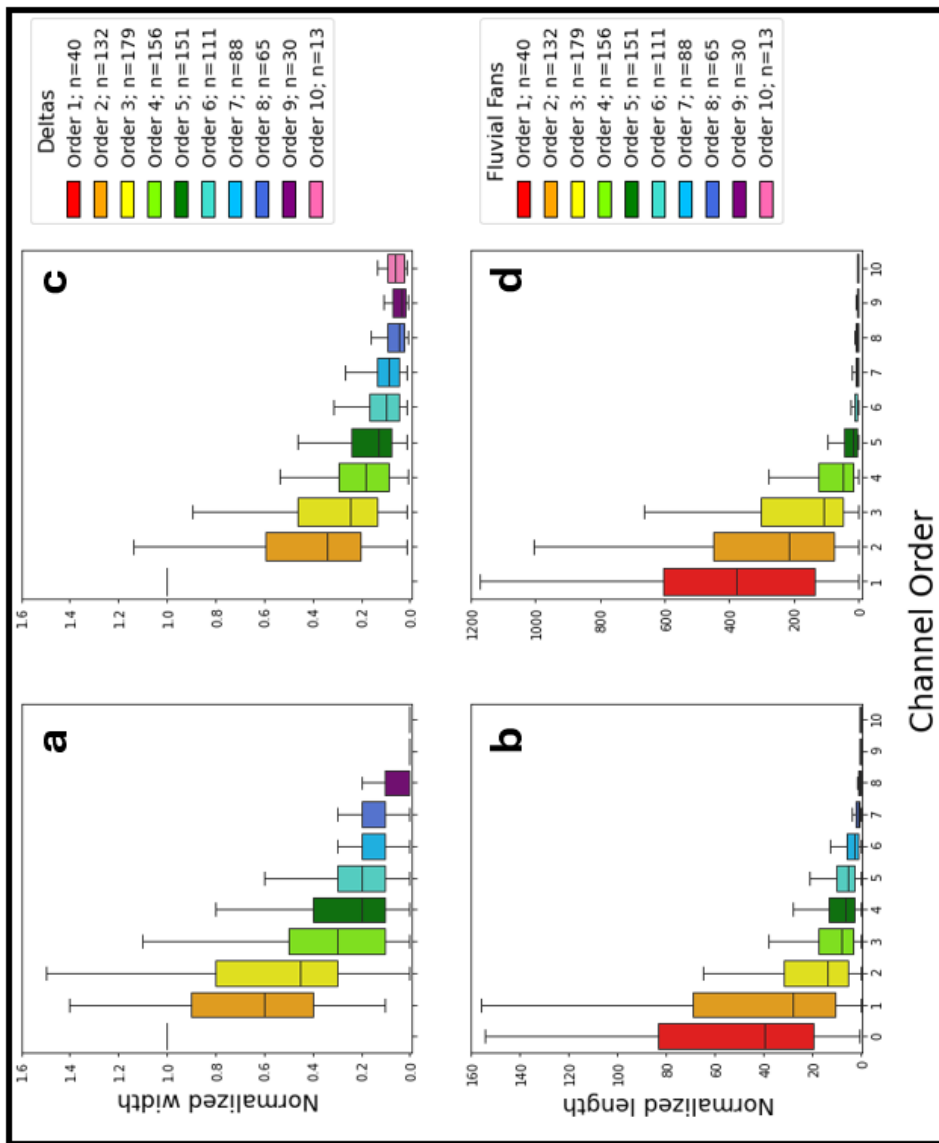


Figure 8: Box and whisker plots illustrating normalized delta channel widths (a) and lengths (b) and normalized fluvial fan channel widths (c) and length (d), plotted by channel order. Note the significant difference in normalized channel length scales for subplots b and d.

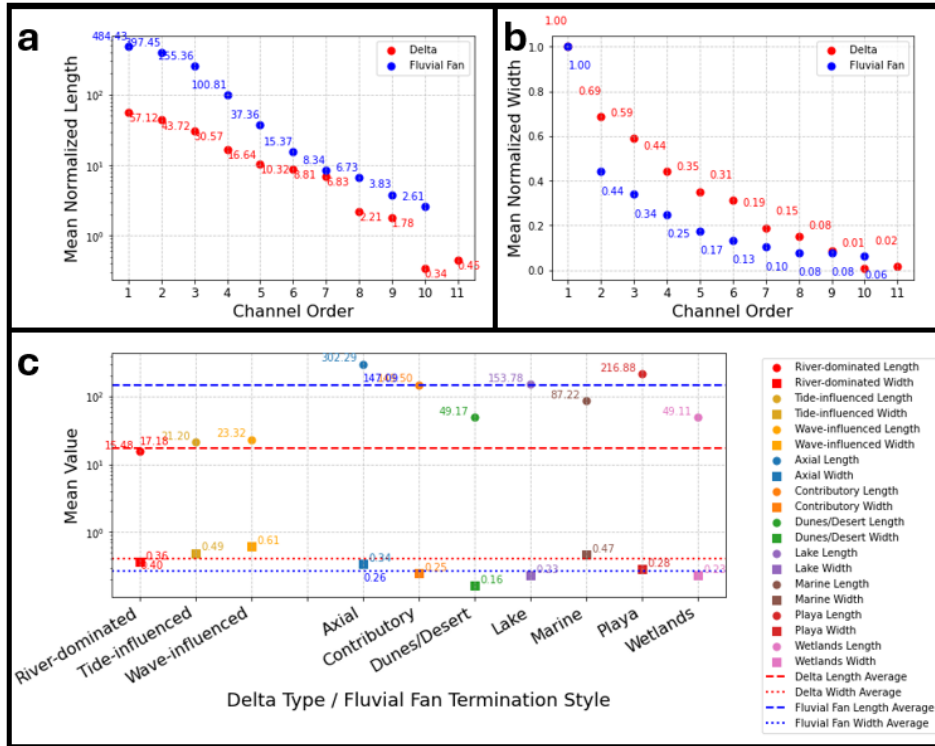


Figure 9: Mean normalized delta and fluvial fan channel (a) lengths by order and (b) width values by order. (c) Mean channel length and width values for different types of deltas and fluvial fan termination styles.

914 Comparison by fluvial fan termination styles shows that axial- and playa-terminating fans exhibit
 915 longer mean normalized channel lengths compared to the whole fluvial fan population, whereas
 916 dunes/desert-, marine-, and wetland-terminating fans have shorter mean lengths (Supplementary Fig. 3
 917 and Supplementary Table 1). Contributory- and lake-terminating fans do not differ significantly from the
 918 overall mean. Regarding normalized channel widths, axial- and marine-terminating fans have wider
 919 channels, while dunes/desert-terminating fans are narrower. Normalized width values for contributory-,
 920 lake-, playa-, and wetland-terminating fan channels show no difference from the overall population mean
 921 (Supplementary Fig. 3 and Supplementary Table 1). Statistical analyses of channel length and width were
 922 not conducted for different fluvial fan termination styles due to insufficient sample sizes ($n < 30$) in most
 923 categories.

924
 925 **5. Discussion**

Deleted: ¶
 Deleted: ,
 Formatted: Indent: First line: 0.25"

Deleted: fans
 Deleted: whole

Deleted: ¶

5.1 Effectiveness of Morphometric Criteria in Distinguishing Deltas and Fluvial Fans

The mean channel network angles are distinctly different in deltas and fluvial fans by 20°, and this statistically significant difference is a useful criterion in distinguishing these two landform types. While some overlaps exist at the landform level, these cases are relatively limited, where 15% of fluvial fans in this dataset have a mean angle larger than 60° (Fig. 5d) and 10% of deltas have a mean angle less than 64° (Fig. 5c). These findings support the utility of mean branching angles as a distinguishing metric between deltas and fluvial fans. However, some degree of uncertainty remains, and additional criteria are necessary for more robust distinction.

An additional criterion is the distribution of mean angles by channel order, where fluvial fans have increased mean angles and a bimodal distribution in orders 4–8 (Fig. 6). Other supportive criteria may be the differences in values and distributions of the normalized channel lengths and widths (Figs. 8 and 9), but the low sample numbers do not allow us to test these criteria by individual landforms. A useful criterion would be to link channel narrowing with the bifurcation and avulsion nodes. In deltas, the downstream channel narrowing occurs in a stepwise manner at the bifurcation nodes, whereas in fluvial fans this decrease should be gradual and not linked to the node positions where full avulsions occur. Our data was collected in a manner that does not permit these analyses.

A potential source of overlap in the delta and fluvial fan channel network mean angles is that not all measured angles in deltas are bifurcation angles, as deltas also experience avulsions (e.g., Fig. 1e). A closer inspection of the four deltas with low mean network angles reveals that each contains very few measurements (n = 3, n = 4, n = 6, n = 7). In these cases, the limited sample size allows the rarer avulsion angles to affect the mean values more strongly. Also, fluvial fans that terminate in a lake or ocean may have terminal channels that form due to mouth bar deposition and channel bifurcation. However, we do not believe these instances affect our results since we do not see that lake- or marine-terminating fans exhibit higher mean angles (Fig. 7d).

Examining fluvial fans with high mean angles shows that these are low-gradient wetland fans, where the avulsion angles tend to be wider as a function of avulsion mechanisms (see Discussion below). However, they may also suggest methodological limitations. While the local avulsion angles in low-gradient wetland fans are wide (measured the final channel width directly upstream of a bifurcation (w_f) as the length for two limbs of an angle), angles between the longer channel reaches are considerably narrower (Supplementary Fig. 4). This channel reach angle discrepancy is consistent with similar channel reach angle measurements from (Coffey & Shaw, 2017). We plan to further develop angle measurement methods to capture both the local and the reach-scale angles in future work. It is also important to discuss the limitations of the applied methodologies in the context of the results. Our channel network methodologies are designed for delta channel networks, and exclude channels that merge downstream,

Deleted: average

Deleted: s

Formatted: Indent: First line: 0.25"

Deleted: n

Deleted: average

Deleted: n

Deleted: average

Deleted: average

Deleted: angle

Deleted: ,

Deleted: though some

Deleted: average

Deleted: s

Deleted: increasing

Deleted: allow

Deleted: us to do thes

Deleted:

Deleted: average

Deleted: average

Deleted: Conversely

Deleted: , h

Deleted: ¶

1023 which can exclude many potential measurements from fluvial fans in situations where their channels
1024 merge downfan.

1025 In summary, this initial attempt to distinguish deltas and fluvial fans demonstrates that quantifying
1026 channel network angles, and trends in normalized channel widths and lengths provide efficient criteria.
1027 However, we also show that sample sizes are important for accurate recognition of landforms, and
1028 collecting a sufficient number of angle measurements ($n \gtrsim 10$) can help account for the infrequent
1029 avulsion in deltas or bifurcation in fluvial fans. While each metric is informative on its own, the
1030 combination of branching angles, branching angle trends, and normalized channel lengths provides the
1031 clearest distinction between deltas and fluvial fans.

1032 5.2 Processes that determine delta and fluvial fan channel network angles

1033 While the 72° mean bifurcation angle can be explained by flow patterns at channel tips well-
1034 explained by diffusive processes (Coffey & Shaw, 2017), there is currently no established explanation for
1035 the approximately 55° mean network angle in fluvial fans. In deltas, bifurcation as a process is the
1036 product of sedimentation from turbulent jets that form at the mouths of rivers entering basins (Bates,
1037 1953; Coffey & Shaw, 2017; Edmonds & Slingerland, 2007; Fagherazzi et al., 2015; Jerolmack &
1038 Swenson, 2007; Wright, 1977). Once a mouth bar is formed, the flow through the distributary channel
1039 bifurcations can be modeled as diffusive flow (Coffey & Shaw, 2017), and the resulting critical angle of
1040 72° represents a stable morphology for the bifurcation as it grows in a diffusive groundwater field
1041 (Devauchelle et al., 2012; Ke et al., 2019). The slightly larger network angles in Arctic deltas may reflect
1042 environmental influences such as ice cover, permafrost, or limitations on overbank flow (Lauzon et al.,
1043 2019; Piliouras et al., 2021; Walker, 1998).

1044 River avulsions are set up by channel superelevation (Mohrig et al., 2000), or when the slope down
1045 the flanks of the channel provides a steeper descent than the existing river channel (Slingerland & Smith,
1046 1998; Törnqvist & Bridge, 2002). Avulsions result from channel bed aggradation that reduces the channel
1047 capacity (Bryant et al., 1995). Once an avulsion is triggered, and full or partial river flow exits the channel,
1048 a new channel is generated by surface runoff erosion. Thus, the prevailing topographic gradient would
1049 tend to keep the nearby flows more focused in a slope-parallel direction, resulting in narrower network
1050 angles compared to bifurcations (Fig. 5b).

1051 The contrast between diffusion-dominated and surface runoff erosion-dominated processes in shaping
1052 delta versus fluvial fan channel network topology is further supported by tributary channel network
1053 analyses that originally defined the critical angle of 72° (Devauchelle et al., 2012). Tributary channel
1054 network analyses show that the mean tributary angle of 72° only occurs in humid catchments with high
1055 groundwater recharge, where tributary networks are shaped by groundwater diffusion (Seybold et al.,

Deleted: s

Deleted: .

Deleted: average

Deleted: has a theoretical explanation in diffusion in non-channelized flow (Coffey & Shaw, 2017)...

Deleted: average

Formatted: Indent: First line: 0.25"

Deleted: ,

Deleted: compared to bifurcations,

Deleted: average

1065 2017). In contrast, the mean tributary network angle is 45° in arid landscapes where surface runoff
1066 dominates (Seybold et al., 2017), or is even lower in the driest catchments (Seybold et al., 2018).

1067 Fluvial fan gradient decreases progressively downstream (e.g. Chakraborty et al., 2010), such that
1068 higher gradients near the fan apex likely generate more acute angles, whereas the very low gradients near
1069 the toe of the fan would allow for wider angles. This trend likely explains the downstream increase in
1070 fluvial fan network angles and the emergence of the second, wider peak in higher order channels (Fig.
1071 6b). Furthermore, avulsion mechanisms have been shown to change from channel superelevation in
1072 upstream river reaches, where river gradients are steeper, to gradient advantage in downstream low-
1073 gradient reaches (Gearon et al., 2024). In these low-gradient zones, crevassing processes can produce
1074 high-angle deviations with the angle values around 90° (Rahman et al., 2022). Avulsion angles above
1075 100° have been measured in meandering rivers on low-gradient floodplains with vegetation (see Rahman
1076 et al., 2022). These effects may be important controls in the fluvial fan channel networks in low-gradient
1077 vegetated wetlands. Reitz & Jerolmack, (2012) show that abandoned paleo-channel reoccupation may
1078 control new avulsion positions, and paleo-channel density is highest in the narrower fan apex. Avulsion
1079 angles may also change over time due to evolving channel width ratios (Morais & Montanher, 2022), or
1080 may be affected by a critical angle or bend curvature (Yang, 2020). Future work targeting how avulsion
1081 morphology evolves downfan would provide important insight into the mechanisms driving the observed
1082 increase in angles downstream.

1083 We thus conclude that the distinction between deltaic and fluvial fan channel network angles arises
1084 from the dominant formative processes: diffusive flow in deltas versus surface runoff erosion in fluvial
1085 fans. Furthermore, in fluvial fans, network angles appear to be negatively correlated with surface
1086 gradients, with lower gradients allowing for wider avulsion angles.

1087 5.3 Ancient deltas and fluvial fans

1088 Our proposed methodology could also be used to distinguish ancient fluvial fans and deltas, for
1089 instance in seismic datasets, where only delta channel network angles have been quantified before
1090 (Mahon et al., 2024). Our results confirm the prior modern data (Chakraborty et al., 2010) and recent
1091 modeling outcomes (Martin & Edmonds, 2023), and help to eliminate a discrepancy in plan-view versus
1092 cross-sectional fluvial fan facies models (Plink-Björklund, 2021). Namely, earlier work suggested
1093 bifurcations as a key mechanism driving fluvial fan formation (Friend, 1978; Kelly & Olsen, 1993;
1094 Weissman et al., 2010), probably due to downstream channel narrowing. However, this hypothesis
1095 contradicts the stratigraphic data that indicate that proximal fans consist of amalgamated channel deposits
1096 (Chakraborty et al., 2010; Kelly & Olsen, 1993; Nichols & Fisher, 2007; Singh et al., 1993; Weissman et
1097 al., 2013) – a pattern consistent with frequent avulsions (Chakraborty et al., 2010; Singh et al., 1993).

1098 5.4 Sensitivity of Deltas and Fluvial Fans to Global Change

Deleted: s average

Deleted: at

Deleted: are

Deleted: (

Deleted: Rahman et al., 2022)

Formatted: Font: (Default) Times New Roman

Deleted: (Mahon et al., 2024)

Deleted: conundrum or

1106 Deltas and fluvial fans differ significantly in their vulnerability to natural hazards and in their
 1107 responses to global change. Deltas are highly vulnerable to coastal hazards and sea level rise (Giosan et
 1108 al., 2014; Syvitski et al., 2009). Rising sea-levels will not only inundate deltaic distributary networks, but
 1109 also cause a landward migration of the avulsion node corresponding with the landward shift of the
 1110 backwater zone (Brooke et al., 2022; Chatanantavet et al., 2012; Ganti et al., 2014). This process reduces
 1111 sediment delivery to shorelines, accelerating the effects of sea-level rise. However, changes in land use
 1112 and changing precipitation patterns which increase sediment supply could complicate the picture by
 1113 shifting delta avulsion sites seaward (Brooke et al., 2022). In contrast, fluvial fans are controlled by
 1114 upstream morphodynamics, where the fan location (apex) is pinned by a steep topographic break (Brooke
 1115 et al., 2022; Ganti et al., 2014; Martin & Edmonds, 2023). For coastal fans, sea-level rise and coastal
 1116 erosion would affect the fan toes, however the avulsion node at the fan apex and sediment deposition
 1117 across most of the fan surface would not be affected, making fluvial fans significantly less vulnerable to
 1118 drowning.

Deleted: (e.g., Syvitski et al., 2009; Giosan et al., 2014).

Deleted: ((Brooke et al., 2022)Ganti et al., 2014; Martin & Edmonds, 2023)

Deleted: While

Deleted: and

Deleted: position,

Deleted: delivery

1119 Both deltas and fluvial fans are affected by reduced sediment supply due to river damming and
 1120 artificial levees (Blum & Roberts, 2009; Giosan et al., 2014; Nienhuis et al., 2020; Paola et al., 2011;
 1121 Syvitski et al., 2009). However, fluvial fans are highly sensitive to the water and sediment supply
 1122 changes, such as changes in precipitation patterns (Assine et al., 2014; Hansford & Plink-Björklund,
 1123 2020; Leier et al., 2005). Increases in extreme precipitation cause a significant increase in avulsion
 1124 frequency and crevassing splay formation (Morón et al., 2017), because large fluctuations in river
 1125 discharge, such as during extreme precipitation events, are avulsion-triggering events (Jones & Schumm,
 1126 1999). Indeed, fluvial fans have been shown to be highly sensitive to such changes, where fluvial fan
 1127 activation and deactivation cycles have been linked to millennial-scale changes in monsoon intensity or
 1128 precipitation patterns (Assine et al., 2014; Fontana et al., 2014, Latrubesse et al., 2012).

Deleted: (e.g., Blum & Roberts, 2009; Syvitski et al., 2009; Giosan et al., 2014; Nienhuis et al., 2020; Paola et al., 2011). ...

Deleted: driven by

Deleted: (Leier et al., 2005; Assine et al., 2014; Hansford & Plink-Björklund, 2020).

Deleted: b

Deleted:

Deleted: (Jones & Schumm, 1999c)

Formatted: Font:

Deleted: ¶

Formatted: Indent: First line: 0.25"

1129 6. Conclusions

1130 This study demonstrates that river-dominated delta and fluvial fan channel networks can be
 1131 distinguished using quantitative morphometric criteria derived from their channel network topology.

Deleted: average

1132 Deltaic networks are primarily shaped by bifurcation processes, resulting in mean bifurcation angles of
 1133 approximately 74°, consistent with diffusion-dominated growth. In contrast, fluvial fan topology is
 1134 shaped by channel avulsions, producing narrower mean network angles near 55°, indicative of surface
 1135 runoff processes. Fluvial fan network angles tend to widen downstream, likely due to decreasing gradients
 1136 and avulsion style shifts, while delta angles remain relatively consistent, reflecting persistent bifurcation
 1137 processes. Both channel networks display downstream reductions in channel length and width with
 1138 increasing channel order, but the fluvial fan networks are characterized by significantly longer and
 1139 somewhat narrower channels when normalized.

Deleted: average

Deleted: ,

1160 These differences not only support the use of network morphology as a diagnostic tool for
1161 identifying ancient fluvial fans and deltas in the stratigraphic record or other planetary bodies but also
1162 provide insights into their differing sensitivities to environmental change.

1163

1164 **Code Availability**

1165 The Python code used for data analysis and figure generation was created and run in Jupyter
1166 Notebook version 6.4.8 (Anaconda distribution).

1167

1168 **Data Availability**

1169 Morphological data collected in this study are available at [https://github.com/lukegezovich/Delta-and-](https://github.com/lukegezovich/Delta-and-Fluvial-Fan-Networks)
1170 [Fluvial-Fan-Networks](https://github.com/lukegezovich/Delta-and-Fluvial-Fan-Networks).

1171

1172 **Competing Interests**

1173 The authors declare that they have no conflict of interest.

1174

1175 **Acknowledgments**

1176 We thank Kamini Singha, Lesli Wood, and Wendy Zhou for their constructive feedback that helped
1177 improve earlier versions of this manuscript. We also thank John Shaw, Ellen Chamberlin and an
1178 anonymous reviewer for their helpful comments on the present versions of the manuscript.

1179

1180 **Financial Support**

1181 Luke Gezovich thanks the American Association of Petroleum Geologists (AAPG) Foundation John &
1182 Erika Lockridge Grant, the American Institute of Professional Geologists (AIPG) William J. Siok Graduate
1183 Scholarship, the Colorado Scientific Society (CSS), the Rocky Mountain Association of Geologists
1184 (RMAG), and the Society for Sediment Geology (SEPM) for providing funding to support this research.

1185

1186

1187

1188

1189

1190

1191

1192

Commented [PP3]: This is confusing as they are not journal reviewers. Also, usually just names are used so I would eliminate "Drs"

Deleted: reviewers Drs

Deleted: .

Formatted: Indent: First line: 0.25"

Deleted: want to

Deleted: Drs.

Deleted: and

Deleted: on later

Deleted: our

Formatted: Indent: First line: 0.25"

Formatted: Line spacing: 1.5 lines

1200

References

- 1201 Allen, P. A. (2008). Time scales of tectonic landscapes and their sediment routing systems. *Geological Society, London, Special Publications*, 296(1), 7–28. <https://doi.org/10.1144/SP296.2>
- 1202
- 1203 Assine, M. L. (2005). River avulsions on the Taquari megafan, Pantanal wetland, Brazil. *Geomorphology*, 70(3–4), 357–371. <https://doi.org/10.1016/j.geomorph.2005.02.013>
- 1204
- 1205 Assine, M. L., Corradini, F. A., Pupim, F. D. N., & McGlue, M. M. (2014). Channel arrangements and depositional styles in the São Lourenço fluvial megafan, Brazilian Pantanal wetland. *Sedimentary Geology*, 301, 172–184. <https://doi.org/10.1016/j.sedgeo.2013.11.007>
- 1206
- 1207
- 1208 Axelsson, V. (1967). The Laitaure Delta: A Study of Deltaic Morphology and Processes. *Geografiska Annaler. Series A, Physical Geography*, 49(1), 1. <https://doi.org/10.2307/520865>
- 1209
- 1210 Bates, C. C. (1953). Rational Theory of Delta Formation. *AAPG Bulletin*, 37. <https://doi.org/10.1306/5CEADD76-16BB-11D7-8645000102C1865D>
- 1211
- 1212 Bentley, S. J., Blum, M. D., Maloney, J., Pond, L., & Paulsell, R. (2016). The Mississippi River source-to-sink system: Perspectives on tectonic, climatic, and anthropogenic influences, Miocene to Anthropocene. *Earth-Science Reviews*, 153, 139–174. <https://doi.org/10.1016/j.earscirev.2015.11.001>
- 1213
- 1214
- 1215 Blair, T. C., & McPherson, J. G. (1994). Alluvial Fans and their Natural Distinction from Rivers Based on Morphology, Hydraulic Processes, Sedimentary Processes, and Facies Assemblages. *SEPM Journal of Sedimentary Research, Vol. 64A*. <https://doi.org/10.1306/D4267DDE-2B26-11D7-8648000102C1865D>
- 1216
- 1217
- 1218 Blum, M. D., & Roberts, H. H. (2009). Drowning of the Mississippi Delta due to insufficient sediment supply and global sea-level rise. *Nature Geoscience*, 2(7), 488–491. <https://doi.org/10.1038/ngeo553>
- 1219
- 1220 Bramble, M. S., Goudge, T. A., Milliken, R. E., & Mustard, J. F. (2019). Testing the deltaic origin of fan deposits at Bradbury Crater, Mars. *Icarus*, 319, 363–366. <https://doi.org/10.1016/j.icarus.2018.09.024>
- 1221
- 1222 Broaddus, C. M., Vulis, L. M., Nienhuis, J. H., Tejedor, A., Brown, J., Foufoula-Georgiou, E., & Edmonds, D. A. (2022). First-Order River Delta Morphology Is Explained by the Sediment Flux Balance From Rivers, Waves, and Tides. *Geophysical Research Letters*, 49(22). <https://doi.org/10.1029/2022GL100355>
- 1223
- 1224
- 1225 Brooke, S., Chadwick, A. J., Silvestre, J., Lamb, M. P., Edmonds, D. A., & Ganti, V. (2022). Where rivers jump course. *Science*, 376(6596), 987–990. <https://doi.org/10.1126/science.abm1215>
- 1226
- 1227 Bryant, M., Falk, P., & Paola, C. (1995). Experimental study of avulsion frequency and rate of deposition. *Geology*, 23(4), 365. [https://doi.org/10.1130/0091-7613\(1995\)023%253C0365:ESOFAFA%253E2.3.CO;2](https://doi.org/10.1130/0091-7613(1995)023%253C0365:ESOFAFA%253E2.3.CO;2)
- 1228
- 1229 Chakraborty, T., Kar, R., Ghosh, P., & Basu, S. (2010). Kosi megafan: Historical records, geomorphology and the recent avulsion of the Kosi River. *Quaternary International*, 227(2), 143–160. <https://doi.org/10.1016/j.quaint.2009.12.002>
- 1230
- 1231
- 1232 Chamberlain, E. L., Törnqvist, T. E., Shen, Z., Mauz, B., & Wallinga, J. (2018). Anatomy of Mississippi Delta growth and its implications for coastal restoration. *Science Advances*, 4(4), eaar4740. <https://doi.org/10.1126/sciadv.aar4740>
- 1233
- 1234

Deleted: ¶



- 1251 Chatanantavet, P., & Lamb, M. P. (2014). Sediment transport and topographic evolution of a coupled
 1252 river and river plume system: An experimental and numerical study: EXPERIMENTS COUPLED RIVER &
 1253 RIVER-PLUME. *Journal of Geophysical Research: Earth Surface*, *119*(6), 1263–1282.
 1254 <https://doi.org/10.1002/2013JF002810>
- 1255 Chatanantavet, P., Lamb, M. P., & Nittrouer, J. A. (2012). Backwater controls of avulsion location on
 1256 deltas. *Geophysical Research Letters*, *39*(1), 2011GL050197. <https://doi.org/10.1029/2011GL050197>
- 1257 Chen, C., Tian, B., Schwarz, C., Zhang, C., Guo, L., Xu, F., Zhou, Y., & He, Q. (2021). Quantifying delta
 1258 channel network changes with Landsat time-series data. *Journal of Hydrology*, *600*, 126688.
 1259 <https://doi.org/10.1016/j.jhydrol.2021.126688>
- 1260 Coffey, T. S., & Shaw, J. B. (2017). Congruent Bifurcation Angles in River Delta and Tributary Channel
 1261 Networks. *Geophysical Research Letters*, *44*(22). <https://doi.org/10.1002/2017GL074873>
- 1262 Davidson, S. K., & Hartley, A. J. (2014). A Quantitative Approach To Linking Drainage Area and
 1263 Distributive-Fluvial-System Area In Modern and Ancient Endorheic Basins. *Journal of Sedimentary
 1264 Research*, *84*(11), 1005–1020. <https://doi.org/10.2110/jsr.2014.79>
- 1265 Davidson, S. K., Hartley, A. J., Weissmann, G. S., Nichols, G. J., & Scuderi, L. A. (2013). Geomorphic
 1266 elements on modern distributive fluvial systems. *Geomorphology*, *180–181*, 82–95.
 1267 <https://doi.org/10.1016/j.geomorph.2012.09.008>
- 1268 De Toffoli, B., Plesa, A. -C., Hauber, E., & Breuer, D. (2021). Delta Deposits on Mars: A Global Perspective.
 1269 *Geophysical Research Letters*, *48*(17), e2021GL094271. <https://doi.org/10.1029/2021GL094271>
- 1270 Devauchelle, O., Petroff, A. P., Seybold, H. F., & Rothman, D. H. (2012). Ramification of stream networks.
 1271 *Proceedings of the National Academy of Sciences*, *109*(51), 20832–20836.
 1272 <https://doi.org/10.1073/pnas.1215218109>
- 1273 Di Achille, G., & Hynek, B. M. (2010). Ancient ocean on Mars supported by global distribution of deltas
 1274 and valleys. *Nature Geoscience*, *3*(7), 459–463. <https://doi.org/10.1038/ngeo891>
- 1275 Dong, T. Y., Nittrouer, J. A., Il'icheva, E., Pavlov, M., McElroy, B., Czapiga, M. J., Ma, H., & Parker, G.
 1276 (2016). Controls on gravel termination in seven distributary channels of the Selenga River Delta, Baikal
 1277 Rift basin, Russia. *Geological Society of America Bulletin*, *128*(7–8), 1297–1312.
 1278 <https://doi.org/10.1130/B31427.1>
- 1279 Donselaar, M. E., Cuevas Gozalo, M. C., & Moyano, S. (2013). Avulsion processes at the terminus of low-
 1280 gradient semi-arid fluvial systems: Lessons from the Río Colorado, Altiplano endorheic basin, Bolivia.
 1281 *Sedimentary Geology*, *283*, 1–14. <https://doi.org/10.1016/j.sedgeo.2012.10.007>
- 1282 Edmonds, D. A., Martin, H. K., Valenza, J. M., Henson, R., Weissmann, G. S., Miltenberger, K., Mans, W.,
 1283 Moore, J. R., Slingerland, R. L., Gibling, M. R., Bryk, A. B., & Hajek, E. A. (2022). Rivers in reverse:
 1284 Upstream-migrating dechannelization and flooding cause avulsions on fluvial fans. *Geology*, *50*(1), 37–
 1285 41. <https://doi.org/10.1130/G49318.1>
- 1286 Edmonds, D. A., Paola, C., Hoyal, D. C. J. D., & Sheets, B. A. (2011). Quantitative metrics that describe
 1287 river deltas and their channel networks. *Journal of Geophysical Research*, *116*(F4), F04022.
 1288 <https://doi.org/10.1029/2010JF001955>

1289 Edmonds, D. A., & Slingerland, R. L. (2007). Mechanics of river mouth bar formation: Implications for the
1290 morphodynamics of delta distributary networks. *Journal of Geophysical Research: Earth Surface*,
1291 *112*(F2), 2006JF000574. <https://doi.org/10.1029/2006JF000574>

1292 ESRI. (2025). *World Imagery* [Imagery layer]. Esri, Maxar.
1293 <https://www.arcgis.com/home/item.html?id=10df2279f9684e4a9f6a7f08febac2a9>

1294 Fagherazzi, S. (2008). Self-organization of tidal deltas. *Proceedings of the National Academy of Sciences*,
1295 *105*(48), 18692–18695. <https://doi.org/10.1073/pnas.0806668105>

1296 Fagherazzi, S., Edmonds, D. A., Nardin, W., Leonardi, N., Canestrelli, A., Falcini, F., Jerolmack, D. J.,
1297 Mariotti, G., Rowland, J. C., & Slingerland, R. L. (2015). Dynamics of river mouth deposits. *Reviews of*
1298 *Geophysics*, *53*(3), 642–672. <https://doi.org/10.1002/2014RG000451>

1299 Farley, K. A., Williford, K. H., Stack, K. M., Bhartia, R., Chen, A., De La Torre, M., Hand, K., Goreva, Y.,
1300 Herd, C. D. K., Hueso, R., Liu, Y., Maki, J. N., Martinez, G., Moeller, R. C., Nelessen, A., Newman, C. E.,
1301 Nunes, D., Ponce, A., Spanovich, N., ... Wiens, R. C. (2020). Mars 2020 Mission Overview. *Space Science*
1302 *Reviews*, *216*(8), 142. <https://doi.org/10.1007/s11214-020-00762-y>

1303 Federici, B., & Paola, C. (2003). Dynamics of channel bifurcations in noncohesive sediments. *Water*
1304 *Resources Research*, *39*(6), 2002WR001434. <https://doi.org/10.1029/2002WR001434>

1305 Fielding, C. R., Ashworth, P. J., Best, J. L., Prokocki, E. W., & Smith, G. H. S. (2012). Tributary, distributary
1306 and other fluvial patterns: What really represents the norm in the continental rock record? *Sedimentary*
1307 *Geology*, *261–262*, 15–32. <https://doi.org/10.1016/j.sedgeo.2012.03.004>

1308 Fontana, A., Mozzi, P., & Marchetti, M. (2014). Alluvial fans and megafans along the southern side of the
1309 Alps. *Sedimentary Geology*, *301*, 150–171. <https://doi.org/10.1016/j.sedgeo.2013.09.003>

1310 Friend, P. F. (1978). *DISTINCTIVE FEATURES OF SOME ANCIENT RIVER SYSTEMS*.

1311 Galloway, E. (1975). Process Framework for Describing the Morphologic and Stratigraphic Evolution of
1312 Deltaic Depositional Systems. *Deltas: Models for Exploration*, 1975, 87–98.

1313 Ganti, V., Chu, Z., Lamb, M. P., Nittrouer, J. A., & Parker, G. (2014). Testing morphodynamic controls on
1314 the location and frequency of river avulsions on fans versus deltas: Huanghe (Yellow River), China.
1315 *Geophysical Research Letters*, *41*(22), 7882–7890. <https://doi.org/10.1002/2014GL061918>

1316 Gearon, J. H., Martin, H. K., DeLisle, C., Barefoot, E. A., Mohrig, D., Paola, C., & Edmonds, D. A. (2024).
1317 Rules of river avulsion change downstream. *Nature*, *634*(8032), 91–95. <https://doi.org/10.1038/s41586-024-07964-2>

1318

1319 Geleynse, N., Storms, J. E. A., Walstra, D.-J. R., Jagers, H. R. A., Wang, Z. B., & Stive, M. J. F. (2011).
1320 Controls on river delta formation; insights from numerical modelling. *Earth and Planetary Science*
1321 *Letters*, *302*(1–2), 217–226. <https://doi.org/10.1016/j.epsl.2010.12.013>

1322 Giosan, L., Syvitski, J., Constantinescu, S., & Day, J. (2014). Climate change: Protect the world's deltas.
1323 *Nature*, *516*(7529), 31–33. <https://doi.org/10.1038/516031a>

1324 Hansford, M. R., & Plink-Björklund, P. (2020). River discharge variability as the link between climate and
1325 fluvial fan formation. *Geology*, *48*(10), 952–956. <https://doi.org/10.1130/G47471.1>

- 1326 Hariharan, J., Piliouras, A., Schwenk, J., & Passalacqua, P. (2022). Width-Based Discharge Partitioning in
 1327 Distributory Networks: How Right We Are. *Geophysical Research Letters*, *49*(14), e2022GL097897.
 1328 <https://doi.org/10.1029/2022GL097897>
- 1329 Harris, C. R., Millman, K. J., van der Walt, S. J., Gommers, R., Virtanen, P., Cournapeau, D., Wieser, E.,
 1330 Taylor, J., Berg, S., Smith, N. J., Kern, R., Picus, M., Hoyer, S., van Kerkwijk, M. H., Brett, M., Haldane, A.,
 1331 del Río, J. F., Wiebe, M., Peterson, P., ... Oliphant, T. E. (2020). Array programming with NumPy. *Nature*,
 1332 *585*(7825), 357–362. <https://doi.org/10.1038/s41586-020-2649-2>
- 1333 Hartley, A. J., Weissmann, G. S., Nichols, G. J., & Warwick, G. L. (2010). Large Distributive Fluvial Systems:
 1334 Characteristics, Distribution, and Controls on Development. *Journal of Sedimentary Research*, *80*(2),
 1335 167–183. <https://doi.org/10.2110/jsr.2010.016>
- 1336 Horton, B. K., & Decelles, P. G. (2001). *Modern and ancient Fluvial megafans in the foreland basin system*
 1337 *of the central Andes, southern Bolivia: Implications for drainage network evolution in fold-thrust belts*
 1338 (pp. 43–63).
- 1339 Hunter, J. D. (2007). MATPLOTLIB - 2D GRAPHICS ENVIRONMENT. *Computing in Science & Engineering*.
- 1340 Isikdogan, F., Bovik, A., & Passalacqua, P. (2017). RivaMap: An automated river analysis and mapping
 1341 engine. *Remote Sensing of Environment*, *202*, 88–97. <https://doi.org/10.1016/j.rse.2017.03.044>
- 1342 Jerolmack, D. J. (2009). Conceptual framework for assessing the response of delta channel networks to
 1343 Holocene sea level rise. *Quaternary Science Reviews*, *28*(17–18), 1786–1800.
 1344 <https://doi.org/10.1016/j.quascirev.2009.02.015>
- 1345 Jerolmack, D. J., & Swenson, J. B. (2007). Scaling relationships and evolution of distributory networks on
 1346 wave-influenced deltas. *Geophysical Research Letters*, *34*(23), 2007GL031823.
 1347 <https://doi.org/10.1029/2007GL031823>
- 1348 Jones, L. S., & Schumm, S. A. (1999). Causes of Avulsion: An Overview. In N. D. Smith & J. Rogers (Eds.),
 1349 *Fluvial Sedimentology VI* (1st ed., pp. 169–178). Wiley. <https://doi.org/10.1002/9781444304213.ch13>
- 1350 Ke, W., Shaw, J. B., Mahon, R. C., & Cathcart, C. A. (2019). Distributory Channel Networks as Moving
 1351 Boundaries: Causes and Morphodynamic Effects. *Journal of Geophysical Research: Earth Surface*, *124*(7),
 1352 1878–1898. <https://doi.org/10.1029/2019JF005084>
- 1353 Kelly, S. B., & Olsen, H. (1993). Terminal fans a review with reference to Devonian examples. In
 1354 *Sedimentary Geology* (Vol. 85, pp. 339–374).
- 1355 Lauzon, R., Piliouras, A., & Rowland, J. C. (2019). Ice and Permafrost Effects on Delta Morphology and
 1356 Channel Dynamics. *Geophysical Research Letters*, *46*(12), 6574–6582.
 1357 <https://doi.org/10.1029/2019GL082792>
- 1358 Leier, A. L., DeCelles, P. G., & Pelletier, J. D. (2005). Mountains, monsoons, and megafans. *Geology*,
 1359 *33*(4), 289. <https://doi.org/10.1130/G21228.1>
- 1360 Leonardi, N., Canestrelli, A., Sun, T., & Fagherazzi, S. (2013). Effect of tides on mouth bar morphology
 1361 and hydrodynamics. *Journal of Geophysical Research: Oceans*, *118*(9), 4169–4183.
 1362 <https://doi.org/10.1002/jgrc.20302>

- 1363 Limaye, A. B., Adler, J. B., Moodie, A. J., Whipple, K. X., & Howard, A. D. (2023). Effect of Standing Water
 1364 on Formation of Fan-Shaped Sedimentary Deposits at Hypanis Valles, Mars. *Geophysical Research*
 1365 *Letters*, 50(4), e2022GL102367. <https://doi.org/10.1029/2022GL102367>
- 1366 Mahon, R., Hughes, C., Chen, H., & Shaw, J. (2024). Ancient Channel-Mouth Bifurcation Angles on Earth
 1367 and Mars. *The Sedimentary Record*, 22(1). <https://doi.org/10.2110/001c.124824>
- 1368 Malin, M. C., & Edgett, K. S. (2015). *Evidence for Persistent Flow and Aqueous Sedimentation on Early*
 1369 *Mars*. www.sciencemag.org
- 1370 Martin, H. K., & Edmonds, D. A. (2023). Avulsion dynamics determine fluvial fan morphology in a cellular
 1371 model. *Geology*, 51(8), 796–800. <https://doi.org/10.1130/G51138.1>
- 1372 Mendenhall, W., Beaver, R. J., & Beaver, B. M. (2012). *Introduction to Probability and Statistics*.
 1373 Brooks/Cole.
- 1374 Mohrig, D., Heller, P. L., Paola, C., & Lyons, W. J. (2000). Interpreting avulsion process from ancient
 1375 alluvial sequences: Guadalope-Matarranya system (northern Spain) and Wasatch Formation (western
 1376 Colorado). *Geological Society of America Bulletin*.
- 1377 Morais, E. S., & Montanher, O. C. (2022). Avulsion in a meandering river: Floodplain conditions for
 1378 occurrence and effects in the parent channel. *CATENA*, 214, 106236.
 1379 <https://doi.org/10.1016/j.catena.2022.106236>
- 1380 Morón, S., Amos, K., Edmonds, D. A., Payenberg, T., Sun, X., & Thyer, M. (2017). Avulsion triggering by El
 1381 Niño–Southern Oscillation and tectonic forcing: The case of the tropical Magdalena River, Colombia. *GSA*
 1382 *Bulletin*, 129(9–10), 1300–1313. <https://doi.org/10.1130/B31580.1>
- 1383 Moscariello, A. (2018). Alluvial fans and fluvial fans at the margins of continental sedimentary basins:
 1384 Geomorphic and sedimentological distinction for geo-energy exploration and development. *Geological*
 1385 *Society, London, Special Publications*, 440(1), 215–243. <https://doi.org/10.1144/SP440.11>
- 1386 Nichols, G. J. (1987). *STRUCTURAL CONTROLS ON FLUVIAL DISTRIBUTARY SYSTEMS-THE LUNA SYSTEM,*
 1387 *NORTHERN SPAIN*.
- 1388 Nichols, G. J., & Fisher, J. A. (2007). Processes, facies and architecture of fluvial distributary system
 1389 deposits. *Sedimentary Geology*, 195(1–2), 75–90. <https://doi.org/10.1016/j.sedgeo.2006.07.004>
- 1390 Nienhuis, J. H., Ashton, A. D., Edmonds, D. A., Hoitink, A. J. F., Kettner, A. J., Rowland, J. C., & Törnqvist,
 1391 T. E. (2020). Global-scale human impact on delta morphology has led to net land area gain. *Nature*,
 1392 577(7791), 514–518. <https://doi.org/10.1038/s41586-019-1905-9>
- 1393 Nienhuis, J. H., Ashton, A. D., & Giosan, L. (2015). What makes a delta wave-dominated? *Geology*, 43(6),
 1394 511–514. <https://doi.org/10.1130/G36518.1>
- 1395 Nienhuis, J. H., Hoitink, A. J. F. T., & Törnqvist, T. E. (2018). Future Change to Tide-Influenced Deltas.
 1396 *Geophysical Research Letters*, 45(8), 3499–3507. <https://doi.org/10.1029/2018GL077638>
- 1397 North, C. P., & Warwick, G. L. (2007). Fluvial Fans: Myths, Misconceptions, and the End of the Terminal-
 1398 Fan Model. *Journal of Sedimentary Research*, 77(9), 693–701. <https://doi.org/10.2110/jsr.2007.072>

- 1399 Olariu, C., & Bhattacharya, J. P. (2006). Terminal distributary channels and delta front architecture of
 1400 river-dominated delta systems. *Journal of Sedimentary Research*, 76(2), 212–233.
 1401 <https://doi.org/10.2110/jsr.2006.026>
- 1402 Ori, G. G., Marinangeli, L., & Baliva, A. (2000). Terraces and Gilbert-type deltas in crater lakes in Ismenius
 1403 Lacus and Memnonia (Mars). *Journal of Geophysical Research: Planets*, 105(E7), 17629–17641.
 1404 <https://doi.org/10.1029/1999JE001219>
- 1405 Owen, A., Nichols, G. J., Hartley, A. J., Weissmann, G. S., & Scuderi, L. A. (2015). Quantification of a
 1406 Distributive Fluvial System: The Salt Wash DFS of the Morrison Formation, SW U.S.A. *Journal of*
 1407 *Sedimentary Research*, 85(5), 544–561. <https://doi.org/10.2110/jsr.2015.35>
- 1408 Paniagua-Arroyave, J. F., & Nienhuis, J. H. (2024). The Quantified Galloway Ternary Diagram of Delta
 1409 Morphology. *Journal of Geophysical Research: Earth Surface*, 129(11), e2024JF007878.
 1410 <https://doi.org/10.1029/2024JF007878>
- 1411 Paola, C., Twilley, R. R., Edmonds, D. A., Kim, W., Mohrig, D., Parker, G., Viparelli, E., & Voller, V. R.
 1412 (2011). Natural Processes in Delta Restoration: Application to the Mississippi Delta. *Annual Review of*
 1413 *Marine Science*, 3(1), 67–91. <https://doi.org/10.1146/annurev-marine-120709-142856>
- 1414 Parker, G., Paola, C., Whipple, K. X., & Mohrig, D. (1998). ALLUVIAL FANS FORMED BY CHANNELIZED
 1415 FLUVIAL AND SHEET FLOW. I: THEORY. *Journal OF Hydraulic Engineering*, 985–995.
- 1416 Passalacqua, P. (2017). The Delta Connectome: A network-based framework for studying connectivity in
 1417 river deltas. *Geomorphology*, 277, 50–62. <https://doi.org/10.1016/j.geomorph.2016.04.001>
- 1418 Pearson, S. G., Van Prooijen, B. C., Elias, E. P. L., Vitousek, S., & Wang, Z. B. (2020). Sediment
 1419 Connectivity: A Framework for Analyzing Coastal Sediment Transport Pathways. *Journal of Geophysical*
 1420 *Research: Earth Surface*, 125(10), e2020JF005595. <https://doi.org/10.1029/2020JF005595>
- 1421 Piliouras, A., Lauzon, R., & Rowland, J. C. (2021). Unraveling the Combined Effects of Ice and Permafrost
 1422 on Arctic Delta Morphodynamics. *Journal of Geophysical Research: Earth Surface*, 126(4),
 1423 e2020JF005706. <https://doi.org/10.1029/2020JF005706>
- 1424 Pizzuto, J. E. (1987). Sediment diffusion during overbank flows. *Sedimentology*, 34(2), 301–317.
 1425 <https://doi.org/10.1111/j.1365-3091.1987.tb00779.x>
- 1426 Plink-Björklund, P. (2021). Distributive Fluvial Systems: Fluvial and Alluvial Fans. In *Encyclopedia of*
 1427 *Geology* (pp. 745–758). Elsevier. <https://doi.org/10.1016/B978-0-08-102908-4.00015-1>
- 1428 Radebaugh, J., Ventra, D., Lorenz, R. D., Farr, T., Kirk, R., Hayes, A., Malaska, M. J., Birch, S., Liu, Z. Y.-C.,
 1429 Lunine, J., Barnes, J., Le Gall, A., Lopes, R., Stofan, E., Wall, S., & Paillou, P. (2018). Alluvial and fluvial fans
 1430 on Saturn’s moon Titan reveal processes, materials and regional geology. *Geological Society, London,*
 1431 *Special Publications*, 440(1), 281–305. <https://doi.org/10.1144/SP440.6>
- 1432 Rahman, M. M., Howell, J. A., & MacDonald, D. I. M. (2022). Quantitative analysis of crevasse-splay
 1433 systems from modern fluvial settings. *Journal of Sedimentary Research*, 92(9), 751–774.
 1434 <https://doi.org/10.2110/jsr.2020.067>

- 1435 Reitz, M. D., & Jerolmack, D. J. (2012). Experimental alluvial fan evolution: Channel dynamics, slope
 1436 controls, and shoreline growth. *Journal of Geophysical Research: Earth Surface*, *117*(F2), 2011JF002261.
 1437 <https://doi.org/10.1029/2011JF002261>
- 1438 Saito, Y., Thanawat, J., Chaimanee, N., Jarupongsakul, T., & Syvitski, J. P. M. (2007). *Shrinking*
 1439 *Megadeltas in Asia: Sea-level Rise and Sediment Reduction Impacts from Case Study of the Chao Phraya*
 1440 *Delta The Holocene Red River Delta, Vietnam View project Global Risks and research priorities for coastal*
 1441 *subsidence View project Shrinking Megadeltas in Asia: Sea-level Rise and Sediment Reduction Impacts*
 1442 *from Case Study of the Chao Phraya Delta*. <https://www.researchgate.net/publication/234045413>
- 1443 Schumm, S. A. (1977). The fluvial system. *Food and Agriculture Organization of the United Nations*.
- 1444 Schwanghart, W., & Kuhn, N. J. (2010). TopoToolbox: A set of Matlab functions for topographic analysis.
 1445 *Environmental Modelling & Software*, *25*(6), 770–781. <https://doi.org/10.1016/j.envsoft.2009.12.002>
- 1446 Seybold, H., Andrade, J. S., & Herrmann, H. J. (2007). Modeling river delta formation. *Proceedings of the*
 1447 *National Academy of Sciences*, *104*(43), 16804–16809. <https://doi.org/10.1073/pnas.0705265104>
- 1448 Seybold, H. J., Kite, E., & Kirchner, J. W. (2018). Branching geometry of valley networks on Mars and
 1449 Earth and its implications for early Martian climate. *Science Advances*, *4*(6), eaar6692.
 1450 <https://doi.org/10.1126/sciadv.aar6692>
- 1451 Seybold, H., Rothman, D. H., & Kirchner, J. W. (2017). Climate’s watermark in the geometry of stream
 1452 networks. *Geophysical Research Letters*, *44*(5), 2272–2280. <https://doi.org/10.1002/2016GL072089>
- 1453 Shaw, J. B., Miller, K., & McElroy, B. (2018). Island Formation Resulting From Radially Symmetric Flow
 1454 Expansion. *Journal of Geophysical Research: Earth Surface*, *123*(2), 363–383.
 1455 <https://doi.org/10.1002/2017JF004464>
- 1456 Singh, H., Parkash, B., & Gohain, K. (1993). Facies analysis of the Kosi megafan deposits. *Sedimentary*
 1457 *Geology*, *85*(1–4), 87–113. [https://doi.org/10.1016/0037-0738\(93\)90077-I](https://doi.org/10.1016/0037-0738(93)90077-I)
- 1458 Sinha, R. (2009). The Great avulsion of Kosi on 18 August 2008. *Current Science*, *97*(3), 429–433.
- 1459 Slingerland, R., & Smith, N. D. (1998). Necessary conditions for a meandering-river avulsion. *Geology*,
 1460 *26*(5), 435. [https://doi.org/10.1130/0091-7613\(1998\)026%253C0435:NCFAMR%253E2.3.CO;2](https://doi.org/10.1130/0091-7613(1998)026%253C0435:NCFAMR%253E2.3.CO;2)
- 1461 Slingerland, R., & Smith, N. D. (2004). RIVER AVULSIONS AND THEIR DEPOSITS. *Annual Review of Earth*
 1462 *and Planetary Sciences*, *32*(1), 257–285. <https://doi.org/10.1146/annurev.earth.32.101802.120201>
- 1463 Smart, J. S. (1971). *QUANTITATIVE PROPERTIES OF DELTA CHANNEL NETWORKS*.
- 1464 Syvitski, J. P. M., & Brakenridge, G. R. (2013). Causation and avoidance of catastrophic flooding along the
 1465 Indus River, Pakistan. *GSA Today*, *23*(1), 4–10. <https://doi.org/10.1130/GSATG165A.1>
- 1466 Syvitski, J. P. M., Kettner, A. J., Overeem, I., Hutton, E. W. H., Hannon, M. T., Brakenridge, G. R., Day, J.,
 1467 Vörösmarty, C., Saito, Y., Giosan, L., & Nicholls, R. J. (2009). Sinking deltas due to human activities.
 1468 *Nature Geoscience*, *2*(10), 681–686. <https://doi.org/10.1038/ngeo629>

1469 Tebolt, M., & Goudge, T. A. (2022). Global investigation of martian sedimentary fan features: Using
1470 stratigraphic analysis to study depositional environment. *Icarus*, 372, 114718.
1471 <https://doi.org/10.1016/j.icarus.2021.114718>

1472 Tejedor, A., Longjas, A., Edmonds, D. A., Zaliapin, I., Georgiou, T. T., Rinaldo, A., & Foufoula-Georgiou, E.
1473 (2017). Entropy and optimality in river deltas. *Proceedings of the National Academy of Sciences*, 114(44),
1474 11651–11656. <https://doi.org/10.1073/pnas.1708404114>

1475 Tejedor, A., Longjas, A., Zaliapin, I., & Foufoula-Georgiou, E. (2015). Delta channel networks: 1. A graph-
1476 theoretic approach for studying connectivity and steady state transport on deltaic surfaces. *Water*
1477 *Resources Research*, 51(6), 3998–4018. <https://doi.org/10.1002/2014WR016577>

1478 Törnqvist, T. E., & Bridge, J. S. (2002). Spatial variation of overbank aggradation rate and its influence on
1479 avulsion frequency. *Sedimentology*, 49(5), 891–905. <https://doi.org/10.1046/j.1365-3091.2002.00478.x>

1480 Trampush, S. M., & Hajek, E. A. (2017). Preserving proxy records in dynamic landscapes: Modeling and
1481 examples from the Paleocene-Eocene Thermal Maximum. *Geology*, 45(11), 967–970.
1482 <https://doi.org/10.1130/G39367.1>

1483 Trauth, M. H. (2006). *MATLAB® Recipes for Earth Sciences*.

1484 Ventra, D., & Clarke, L. E. (2018). Geology and geomorphology of alluvial and fluvial fans: Current
1485 progress and research perspectives. *Geological Society, London, Special Publications*, 440(1), 1–21.
1486 <https://doi.org/10.1144/SP440.16>

1487 Virtanen, P., Gommers, R., Oliphant, T. E., Haberland, M., Reddy, T., Cournapeau, D., Burovski, E.,
1488 Peterson, P., Weckesser, W., Bright, J., van der Walt, S. J., Brett, M., Wilson, J., Millman, K. J., Mayorov,
1489 N., Nelson, A. R. J., Jones, E., Kern, R., Larson, E., ... Vázquez-Baeza, Y. (2020). SciPy 1.0: Fundamental
1490 algorithms for scientific computing in Python. *Nature Methods*, 17(3), 261–272.
1491 <https://doi.org/10.1038/s41592-019-0686-2>

1492 Vulis, L., Tejedor, A., Ma, H., Nienhuis, J. H., Broaddus, C. M., Brown, J., Edmonds, D. A., Rowland, J. C., &
1493 Foufoula-Georgiou, E. (2023). River Delta Morphotypes Emerge From Multiscale Characterization of
1494 Shorelines. *Geophysical Research Letters*, 50(7), e2022GL102684.
1495 <https://doi.org/10.1029/2022GL102684>

1496 Walker, H. J. (1998). Arctic Deltas. *Journal of Coastal Research*, 14(3), 718–738.

1497 Wall, S., Hayes, A., Bristow, C., Lorenz, R., Stofan, E., Lunine, J., Le Gall, A., Janssen, M., Lopes, R., Wye,
1498 L., Soderblom, L., Paillou, P., Aharonson, O., Zebker, H., Farr, T., Mitri, G., Kirk, R., Mitchell, K.,
1499 Notarnicola, C., ... Ventura, B. (2010). Active shoreline of Ontario Lacus, Titan: A morphological study of
1500 the lake and its surroundings. *Geophysical Research Letters*, 37(5), 2009GL041821.
1501 <https://doi.org/10.1029/2009GL041821>

1502 Wang, J., & Plink-Björklund, P. (2019). Stratigraphic complexity in fluvial fans: Lower Eocene Green River
1503 Formation, Uinta Basin, USA. *Basin Research*, 31(5), 892–919. <https://doi.org/10.1111/bre.12350>

1504 Waskom, M. (2021). seaborn: Statistical data visualization. *Journal of Open Source Software*, 6(60), 3021.
1505 <https://doi.org/10.21105/joss.03021>

1506 Weissman, G. S., Hartley, A. J., Nichols, G. J., Scuderi, L. A., Olson, M., Buehler, H., & Banteah, R. (2010).
1507 *Fluvial form in modern continental sedimentary basins: Distributive fluvial systems*.
1508 <https://doi.org/10.1016/j.geo>

1509 Weissmann, G. S., Hartley, A. J., Nichols, G. J., Scuderi, L. A., Olson, M., Buehler, H., & Banteah, R. (2010).
1510 *Fluvial form in modern continental sedimentary basins: Distributive fluvial systems*. *Geology*, *38*(1), 39–
1511 42. <https://doi.org/10.1130/G30242.1>

1512 Weissmann, G. S., Hartley, A. J., Scuderi, L. A., Nichols, G. J., Owen, A., Wright, S., Felicia, A. L., Holland,
1513 F., & Anaya, F. M. L. (2015). Fluvial geomorphic elements in modern sedimentary basins and their
1514 potential preservation in the rock record: A review. *Geomorphology*, *250*, 187–219.
1515 <https://doi.org/10.1016/j.geomorph.2015.09.005>

1516 Witek, P. P., & Czechowski, L. (2015). Dynamical modelling of river deltas on Titan and Earth. *Planetary*
1517 *and Space Science*, *105*, 65–79. <https://doi.org/10.1016/j.pss.2014.11.005>

1518 Wolinsky, M. A., Edmonds, D. A., Martin, J., & Paola, C. (2010). Delta allometry: Growth laws for river
1519 deltas. *Geophysical Research Letters*, *37*(21), 2010GL044592. <https://doi.org/10.1029/2010GL044592>

1520 Wood, L. J. (2006). Quantitative geomorphology of the Mars Eberswalde delta. *Geological Society of*
1521 *America Bulletin*, *118*(5–6), 557–566. <https://doi.org/10.1130/B25822.1>

1522 Wright, L. D. (1977). Sediment transport and deposition at river mouths: A synthesis. *Geological Society*
1523 *of America Bulletin*, *88*(6), 857. [https://doi.org/10.1130/0016-](https://doi.org/10.1130/0016-7606(1977)88%253C857:STADAR%253E2.0.CO;2)
1524 [7606\(1977\)88%253C857:STADAR%253E2.0.CO;2](https://doi.org/10.1130/0016-7606(1977)88%253C857:STADAR%253E2.0.CO;2)

1525 Xu, Z., & Plink-Björklund, P. (2023). Quantifying Formative Processes in River- and Tide-Dominated
1526 Deltas for Accurate Prediction of Future Change. *Geophysical Research Letters*, *50*(20), e2023GL104434.
1527 <https://doi.org/10.1029/2023GL104434>

1528 Yang, H. (2020). Numerical investigation of avulsions in gravel-bed braided rivers. *Hydrological*
1529 *Processes*, *34*(17), 3702–3717. <https://doi.org/10.1002/hyp.13837>

1530